

UNIVERSITY OF TARTU
INSTITUTE OF ECOLOGY AND EARTH SCIENCES
DEPARTMENT OF GEOLOGY

Marija Dmitrijeva

Gravity and magnetic study of the Luusika potential field anomaly

MSc thesis

Supervisors:

Jüri Plado

Tõnis Oja

Tartu 2015

Table of contents

Table of contents	2
Introduction	3
1 Background	4
1.1 Geological setting.....	4
1.2 Crustal domains of Estonian Precambrian basement	4
Metamorphic complexes	4
Syn- , post- and late-orogenic intrusions.....	7
Unorogenic intrusions	8
1.3 Research problem definition and objectives	9
2. Methods and data	12
2.1 Ground magnetic survey	12
2.2 Modeling	13
3. Results	16
3.1 Depth Estimations	16
3.2 Bouguer anomaly	18
3.3 Magnetic anomaly	20
3.4 Geological models.....	22
Taadikvere-like model.....	22
Abja-like model.....	25
Sigula-like model	28
Riga plagioclase porphyry-like model	31
4 Discussion	34
5. Conclusion.....	36
Acknowledgments	37
References	38
Luusika gravitatsiooni- ja magnetväljaanomaalia uuringud	41
Appendices.....	42

Introduction

Geophysical data provide information about geological features which are hidden under the overburden and thus are not observable by conventional geological mapping. Previous geophysical mapping of Estonian basement rocks has revealed gravity and magnetic anomalies produced by various rock types, however in some cases geophysical data were supported by drill holes.

About 10 km wide local maximum (+6.3 mGal) in Bouguer anomaly field were discovered in Luusika (in northeastern Estonia) from the gravity survey data of Estonian Land Board in 2011-2012. No deep drillings has been performed in this area. The airborne magnetic data (1: 25 000) slightly covers the northern side of the Luusika area but no magnetic anomalies are resolved.

The aim of this project is:

- i) Measure magnetic field intensity from the ground within the gravimetrically defined area
- ii) Characterize the potential field anomalies
- iii) Compile the geological models based on geophysical data testing the lithologies of Estonian basement rocks.

The ground magnetic measurements confirmed existing gravity data and resolved the anomalies in more detail. Consequently, the calculations were performed in order to estimate the depth to the top (z_t) of causative source and maximum limiting depth (z).

Geological models were constructed and evaluated in *ModelVision 14.0*. The modeling process was user controlled: the density and magnetic susceptibility were altered by author until a reasonable fit between the response of the model and measured data was obtained. Simulated gravimetric and magnetic response was compared to the corresponding observation data from Luusika area.

In the process of modeling no unique solution to the data exists and, as a result, several different models can be produced to match the same dataset. Four different geological models with different properties were constructed. Models were simulating the post-orogenic Taadikvere intrusion, anorogenic Abja and Sigula massifs, as well as Riga pluton plagioclase porphyry. Derived geological models allowed to determine the range of petrophysical properties for Luusika rock unit and discuss its possible origins.

1 Background

1.1 Geological setting

Estonia is located on the southeastern slope of the Fennoscandian Shield within the Svecofennian domain. During the collision of Volgo-Sarmatia and Fennoscandia between 1.95 ... 1.85 Ga, the growth of the Svecofennian domain occurred as episodes of continental crust accretion (Bogdanova et al., 2015). The Svecofennian orogeny is divided into Lapland-Savo, Fennian, Svecobaltic, and Nordic orogenic zones (Lahtinen et al., 2008; Bogdanova et al., 2008). The accretion of the arc complexes to the pre-existing Archean craton produced over-thickened lithospheric crust represented by belt-shaped structural domains of granulite and amphibolite facies in Belarus, Estonia, Latvia, Lithuania, and Poland (Bogdanova et al., 2015). Between 1.65 and 1.51 Ga the reworking of Svecofennian crust occurred due to the intrusion of rapakivi granites and related rocks (Nironen, 1997).

Radiogenic studies of Northern Estonia complexes revealed ages 1.8 ... 1.9 Ga, which correspond to supracrustal rocks of Fennian orogeny in Southern Finland as well as U-Pb zircon ages of Western and Southern Estonia correspond to Svecobaltic orogeny in Southeastern Sweden (Kirs et al., 2009). Geological studies of crystalline basement in Estonia, Sweden, and Finland have however shown that their basement-forming rocks have many comparable aspects whereas the Estonian crystalline basement is completely covered by 100 ... 800 m of Neoproterozoic and Paleozoic sedimentary rocks (Kirs et al., 2009). Detailed studies of Precambrian basement in Estonia have been carried out through approximately 500 deep boreholes whereas geological investigations have often been combined with potential field interpretations (Puura et al., 1997; All et al., 2004).

Based on above-described studies, the Estonian crystalline basement is presented by (i) amalgamated Paleoproterozoic microcontinents and orogenic belts (Svecofennian metamorphic and plutonic rocks) and (ii) unorogenic complex of rapakivi and related granites. Within Estonia, the Svecofennian crust is approximately 45...65 km thick and is divided (All et al., 2004) into upper and partially upthrusted lower crust.

1.2 Crustal domains of Estonian Precambrian basement

Metamorphic complexes

According to various geological and geophysical studies, Estonian basement is subdivided into six petrological-structural domains: Alutaguse, Jõhvi, Tallinn, Tapa, South Estonia, and

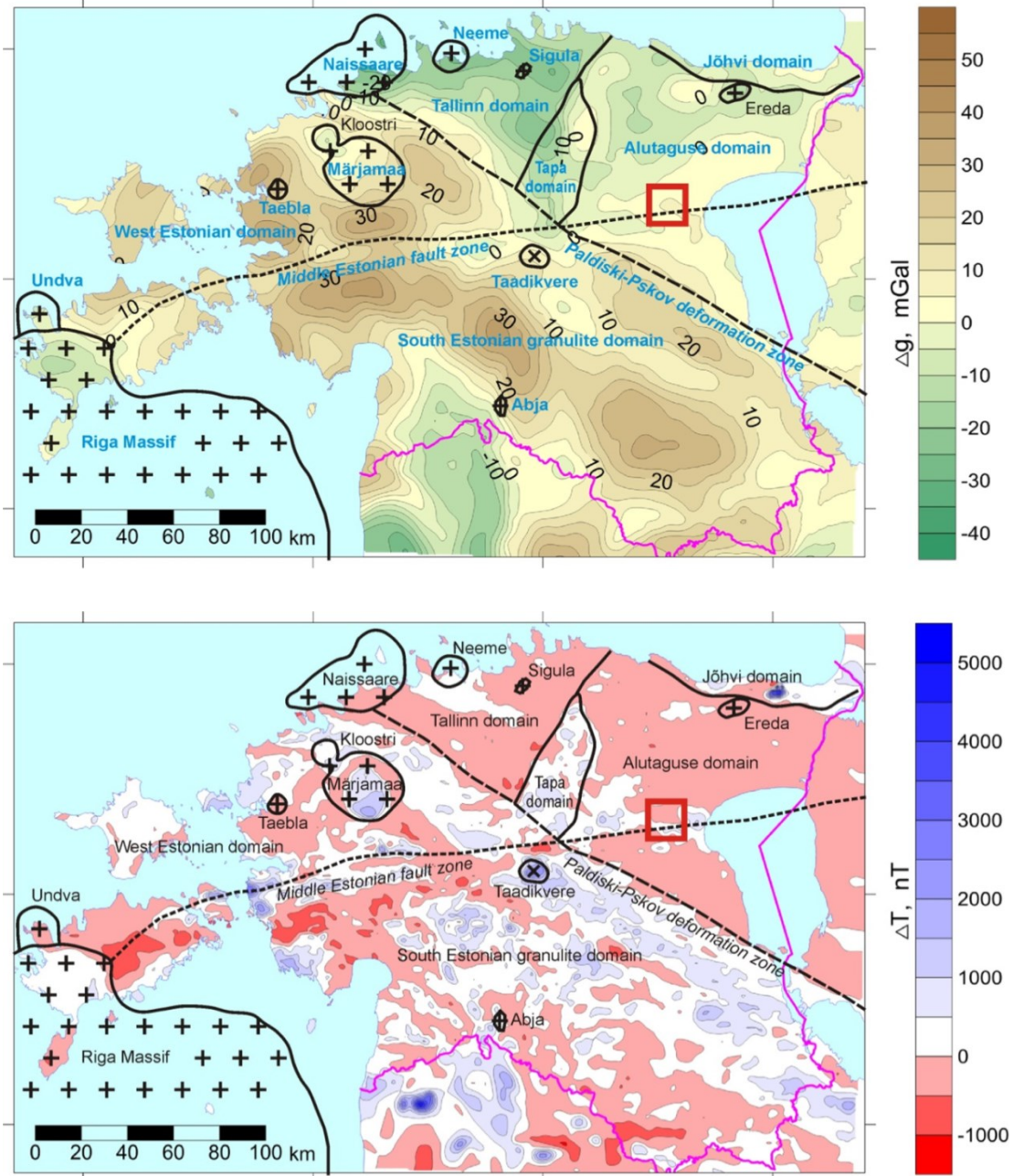


Figure 1. Structural features and metamorphic complexes of Precambrian basement compared to Bouguer gravity (above) and magnetic (below) anomaly maps. Non-marked areas represent Svecofennian metamorphic and plutonic rocks; crossed areas are unorogenic complexes of rapakivi and related (Taadikvere, see text) granites. Geological data are after Puura et al., (1997) and Bogdanova et al., (2015). Geophysical data are by Geological Survey of Estonia (<http://www.egk.ee/asutusest/stuktuur/meregeoloogia-ja-geofuusika>).

West Estonia (Figure 1). Each complex is characterized by specific assemblage of metamorphic rocks and different distribution of metasediments and metavolcanites. The Tapa, Tallinn, and Alutaguse zones are distinguished from other structural zones by predominantly amphibolite facies of metamorphism that passes towards granulite facies (Bogdanova et al., 2015).

Contrasting petrophysical properties of the tectonic domains are reflected in gravity and magnetic maps. The regional high-gradient gravity and magnetic intensities in southern Estonia represent the granulite facies, whereas calm gravity and magnetic signatures of northern Estonia correspond to amphibolite facies (Koppelmaa, 2002; All et al., 2004; Soesoo et al., 2004; Kirs et al., 2009).

The metasedimentary **Alutaguse domain** is derived from clastic successions, probably turbidites, representing deformed and strongly folded marginal part of sedimentary basin extending to the St. Petersburg and Novgorod areas (All et al., 2004; Bogdanova et al., 2015). The metamorphic alumogneisses ($\bar{\rho} = 2680 \dots 2690 \text{ kg/m}^3$; magnetic susceptibility $\bar{\chi} = 10 \dots 138 \times 10^{-6} \text{ SI}$) of amphibolite facies containing biotite, sillimanite, garnet, and cordierite, is defined by low-gradient magnetic field and smooth gravity field. The signatures of granulite facies occur at Sonda-Uljaste, Assamalla, and Haljala areas, and show slightly positive potential field anomalies (Koppelmaa, 2002; All et al., 2004; Soesoo et al., 2004).

Jõhvi domain is a sequence represented by magnetite bearing quartzites, pyroxene- amphibole-biotite gneisses and garnet-cordierite-sillimanite gneisses ($\bar{\rho} = 2850 \text{ kg/m}^3$; $\bar{\chi} = 39 \dots 606 \times 10^{-6} \text{ SI}$). These metamorphic rocks are migmatized by plagioclase-potassium feldspar granites ($\bar{\rho} = 2670 \dots 2680 \text{ kg/m}^3$; $\bar{\chi} = 1 \dots 6.3 \times 10^{-6} \text{ SI}$) and charnockite leucosomes (Soesoo et al., 2004; Bogdanova et al., 2015). Magnetite quartzites within Jõhvi zone ($\bar{\rho} = 3470 \text{ kg/m}^3$; $\bar{\chi} = 4740 \times 10^{-6} \text{ SI}$) are defined by sharp E-W-trending positive magnetic anomaly of more than 13,000 nT in intensity (Koppelmaa, 2002; All et al., 2004).

Tallinn domain is bordered by regional Paldiski-Pskov deformation zone in the south and Tapa domain in the south-east. The zone is characterized by negative magnetic (-100 ... -500 nT) and Bouguer (-26 ... -40 mGal) anomalies. The domain is predominantly formed by folded volcanic rocks, most likely originating from volcanic arc (All et al., 2004), which continues as the Uusimaa tectonic domain in southern Finland (Bogdanova et al., 2015). The metavolcanites and metasediments of amphibolite facies are represented by biotite-plagioclase gneisses ($\bar{\rho} = 2730 \text{ kg/m}^3$; $\bar{\chi} = 6 \times 10^{-6} \text{ SI}$), amphibole-quartz-feldspar gneisses ($\bar{\rho} = 2630 \dots 2760 \text{ kg/m}^3$; $\bar{\chi} = 1.1 \dots 2.5 \times 10^{-6} \text{ SI}$), mica gneisses and less prevalent sulphide-graphite ($\bar{\rho} = 2720 \text{ kg/m}^3$; $\bar{\chi} = 38 \times 10^{-6} \text{ SI}$) and magnetite quartzites ($\bar{\rho} = 3210 \text{ kg/m}^3$; $\bar{\chi} = 1950 \times 10^{-6} \text{ SI}$; Koppelmaa, 2002; Soesoo et al., 2004).

The rocks of **Tapa zone** reveal positive magnetic (up to 500 nT) and Bouguer anomalies (10 ... 15 mGal; Figure 1). Zone is bordered by tectonic contacts from the Alutaguse in the east

and Tallinn domain in the west (All et al., 2004). The domain consists of migmatized amphibolites ($\bar{\rho} = 2960 \text{ kg/m}^3$; $\bar{\chi} = 29 \times 10^{-6} \text{ SI}$) and amphibole gneisses ($\bar{\rho} = 2740 \text{ kg/m}^3$; $\bar{\chi} = 31 \times 10^{-6} \text{ SI}$) representing granulite and amphibolite metamorphic facies. Pyroxene gneisses and biotite-plagioclase gneisses ($\bar{\rho} = 2690 \text{ kg/m}^3$; $\bar{\chi} = 33 \times 10^{-6} \text{ SI}$) are less common, as well as small syn-orogenic gabbro and gabbro-norite ($\bar{\rho} = 2900 \text{ kg/m}^3$; $\bar{\chi} = 62 \times 10^{-6} \text{ SI}$) bodies. For the most part, rocks are mineralogically equivalent to the western Estonia zone, but no contact with it is certainly estimated (Koppelmaa et al., 2002; Puura et al., 1997).

The metasedimentary rocks of **the west Estonia zone** are characterized by high-temperature amphibolite and granulite facies. The domain appears between E-W trending Middle Estonian fault zone and NW-striking Paldiski-Pskov deformational zone (Figure 1; Bogdanova et al., 2015). The complex consists of amphibole gneisses ($\bar{\rho} = 2790 \text{ kg/m}^3$; $\bar{\chi} = 77 \times 10^{-6} \text{ SI}$) and amphibolites ($\bar{\rho} = 2960 \text{ kg/m}^3$; $\bar{\chi} = 49 \times 10^{-6} \text{ SI}$) in association with biotite-feldspar ($\bar{\rho} = 2700 \text{ kg/m}^3$; $\bar{\chi} = 119 \times 10^{-6} \text{ SI}$), quartz-feldspar gneisses ($\bar{\rho} = 2650 \text{ kg/m}^3$; $\bar{\chi} = 46 \times 10^{-6} \text{ SI}$) and minor pyroxene gneisses ($\bar{\rho} = 2800 \text{ kg/m}^3$; $\bar{\chi} = 160 \times 10^{-6} \text{ SI}$) with plagioclase-potassium feldspar granite ($\bar{\rho} = 2650 \text{ kg/m}^3$; $\bar{\chi} = 18 \times 10^{-6} \text{ SI}$) migmatization. Magnetic anomalies are linear and predominantly NE-SE striking whereas intensive gravity anomalies have mosaic character (All et al., 2004; Koppelmaa et al., 2002). Western Estonia domain is also host for several Proterozoic tectonic shear zones (Soesoo et al., 2004).

The metamorphic domain of granulite facies in **south Estonian zone** is dominated by metaigneous granulites varying from felsic to mafic in composition. Sequence is characterized by amphibole-pyroxene gneisses ($\bar{\rho} = 2940 \text{ kg/m}^3$; $\bar{\chi} = 285 \times 10^{-6} \text{ SI}$), and quartz-feldspar gneisses ($\bar{\rho} = 2630 \text{ kg/m}^3$; $\bar{\chi} = 3.3 \times 10^{-6} \text{ SI}$) containing hypersthene, garnet, accessory spinel, sillimanite, and cordierite. The south Estonian domain, however is, recorded geophysically by aligned E-W and NW-trending positive magnetic anomalies (up to 3000 nT) and mosaic-type gravity anomalies extending southwards (Soesoo et al., 2004; Bogdanova et al., 2015).

Syn-, post- and late-orogenic intrusions

The island arc volcanism of Svecofennian orogeny culminated around 1.9 ... 1.86 Ga and compressional tectonics produced high-grade granulite-charnockite belts in Estonia, Latvia and Lithuania as well as syn-orogenic granitoids (Bogdanova et al., 2015). The syn-orogenic granitoids are less distributed. They are known in about 50 drill cores, mostly from Tallinn and Jõhvi zones. Granitoids appear as small bodies, dominated by gneissic structure, consisting of hypersthene-bearing charnockites, granodiorites, and, sometimes, quartz diorites (Puura et al.,

1997; Soesoo et al., 2004). Ultramafic syn-orogenic rocks are distinguished in Alutaguse and South Estonian granulite domains as small peridotite veins in Haljala area and serpentinized peridotite veins are noticed in Otepää drill core (Koppelmaa, 2002).

The compressional stage was followed by isostatic uplift, erosion, thinning and extension of Svecfennian crust. This led to the partial melting of the supracrustal rocks and the formation of late-tectonic migmatite associated granitoids around 1.85 ... 1.80 Ga (Koistinen, 1996; Nironen, 1997). Late-orogenic granitoids are mostly S-type granites occurring in all structural domains of Estonian basement (Niin, 1997). The late-orogenic granitoids and intermediate intrusions were revealed in more than 300 drill cores in all structural domains, but less in granulitic complexes of Jõhvi and Southern Estonia. The intrusions are mainly characterized by felsic metavolcanic rocks, metagabbro-diorites, and metadiorites. They appear as migmatite veins or massifs up to 10 km in diameter. The geophysical responses of the late-orogenic granites are gravity and magnetic minimums (Koppelmaa, 2002).

Due to the erosion of the Earth's surface after the crust thickening and mountain building, post-orogenic granitoids intruded at near-surface conditions (Puura and Flodén, 1999). Mostly, magmatism was related to late-orogenic shears in the south Finland and Estonia (Puura and Flodén, 2000) and, as a result, the distribution of post-orogenic granitoids in the Estonian and Finish basement is quite limited (Niin, 1997). They are represented by partly gneissic quartz-monzonitic and granodioritic rocks and rarely by lamprophyre dykes. Muhu massif, Virtu body with diameter of 3 ... 4 km and Taadikvere body with diameter of 7 ... 8 km are classified to be post-orogenic. On the magnetic map Taadikvere massif appears as a strong magnetic anomaly (Figure 1).

Unorogenic intrusions

The intrusion of rapakivi granites and associated rocks between 1.65 ... 1.50 Ga into preexisting 55 ... 80 km thick Svecfennian domain was a process of stabilizing the overthickened portion of the crust (Puura and Flodén, 1999). On the other hand, the occurrence of rapakivi might be explained by upwelling of the mantle plume material (Haapala et al., 2005).

Extensive igneous activity formed three major rapakivi Subprovinces: the Vyborg-Estonia group (1.62 ... 1.65 Ga), the Åland-Riga group (1.54 ... 1.58 Ga) and the Salmi group (1.54 ... 1.56 Ga) (Koistinen, 1996). Typically, the province is composed of several types of rapakivi located in the central position of the province and satellite mafic massifs around. Those satellite mafic dike swarms and minor massifs are located in the peripheral parts (Puura and

Flodén, 2000). The bimodal nature of rapakivi complexes is explained by partial melting of lower and middle continental crust and of upper mantle (Koistinen, 1996). In Estonia, granite-granodiorite massifs of Naissaare, Neeme, Ereda, Märjamaa, and Taebla, quartz monzodiorite of Abja massif and gabbro-diabase of Sigula massif belong to the Vyborg age group (Koistinen, 1996).

Geophysical patterns of rapakivi rocks of Estonia are varying. They have expressions of negative or positive magnetic and negative gravity anomalies due to variable physical properties. As example, Märjamaa pluton is represented by “granodioritic” rapakivi granite in the center which produce strong positive magnetic anomaly. It is surrounded by a rim of negative magnetic anomaly produced by more felsic rapakivi (Figure 1; Koppelmaa, 2002). Positive magnetic anomalies are also produced by Sigula and Abja massifs (Koistinen, 1996).

1.3 Research problem definition and objectives

Basic and intermediate intrusions are widely distributed within Estonian basement. As it has been introduced above, some of them could be the source of potential field anomalies depending on density and magnetic susceptibility contrast between hosting rock and intrusion. The detailed gravimetric survey conducted by Department of Geodesy of Estonian Land Board in 2010 and 2011 revealed gravimetrically anomalous area in Ida-Virumaa County (Figure 2; Bloom and Oja, 2010; Oja, 2011).

The local uplift of gravity anomaly was recorded in Luusika bog region with coordinates 6 539 337 N; 650 355 E (L-EST97) of center. The gravity survey data were processed by Estonian Land Board. The Bouguer anomaly map (Figure 3) was computed from a free-air anomaly map by computationally removing from it the attraction of the terrain with density of 2300 kg/m^3 . The terrain was approximated by a flat plate of thickness H , which indicates distance between geoid and Earth’s topographic surface. Filtering of long-wave component has produced residual Bouguer anomaly characterizing only the Luusika gravity uplift ranging from -0.8 to 6.3 mGal in amplitude. For the computation of free-air anomalies a normal gravity of GRS-80 ellipsoid was used (also called as a latitude correction).

The aeromagnetic map (1 : 25 000) produced by PGO “Nevskgeologia” between 1987 and 1992 has not fully covered Luusika region.

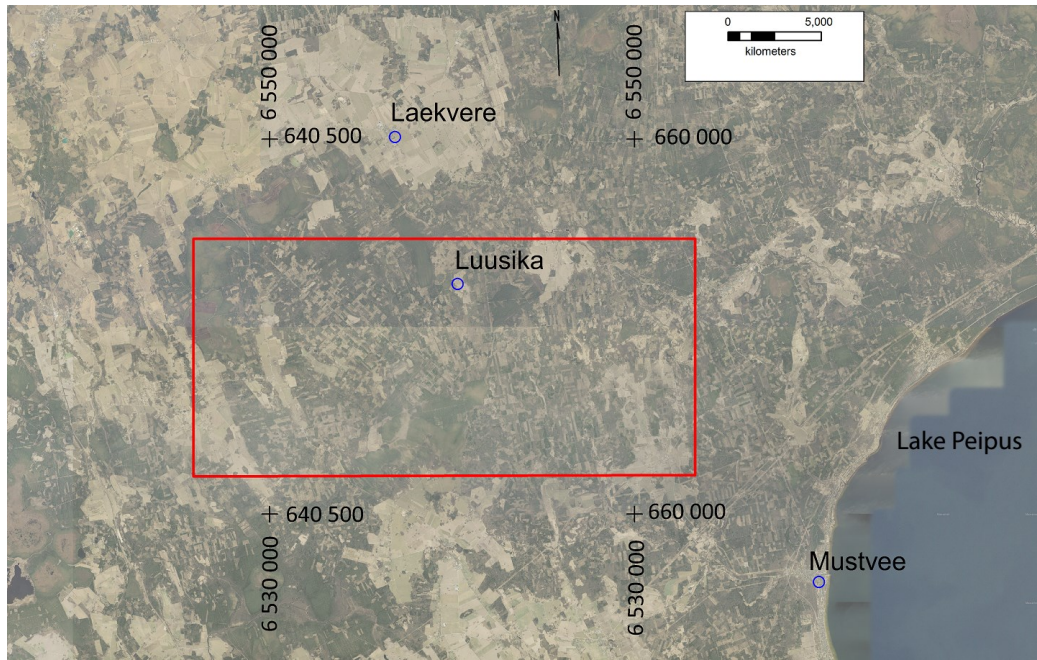


Figure 2. The Luusika area under study is located next to the Lake Peipus. Red rectangular area refers to the position of study area. The data are from Estonian Land Board.

The aim of aeromagnetic survey was to provide information on major crustal structures, study the contours of the crystalline bedrock and, also, spot the local magnetic anomalies possibly produced by kimberlite and lamproite pipes. Measurements were taken by proton-precession magnetometer at altitude 100 m with resolution 1 nT and survey-line spacing 250 m (All, 1995).

Collected data extended across the northern part of the Luusika region; it did not however reveal magnetically anomalous area in this region (Figure 4).

The Luusika region lies within unexposed metasedimentary Alutaguse domain with average density $\bar{\rho} = 2680 \text{ kg/m}^3$ and magnetic susceptibility $\bar{\chi} = 138 \times 10^{-6} \text{ SI}$. There are several types of geologically different bodies within Alutaguse zone documented (Koppelmaa, 2002), such as syn-orogenic gabbro, pyroxene gneiss, pyroxene skarn, marmor, quartzite, late-orogenic granites, migmatites, and unorogenic Ereda rapakivi intrusion. Precambrian basement is covered by 280 ... 300 m thick layer of Ediacaran up to Llandovery sedimentary rocks.

As there are no deep drillings at the Luusika anomaly performed, the source of gravity anomaly remains unclear. The aim of current master's thesis is thus: (i) to obtain a better control over the magnetic field by measuring it from ground, (ii) to characterize the potential (gravity and magnetic) fields and (iii) to create geological models to examine the possible origin of the Luusika source body as based on potential field data.

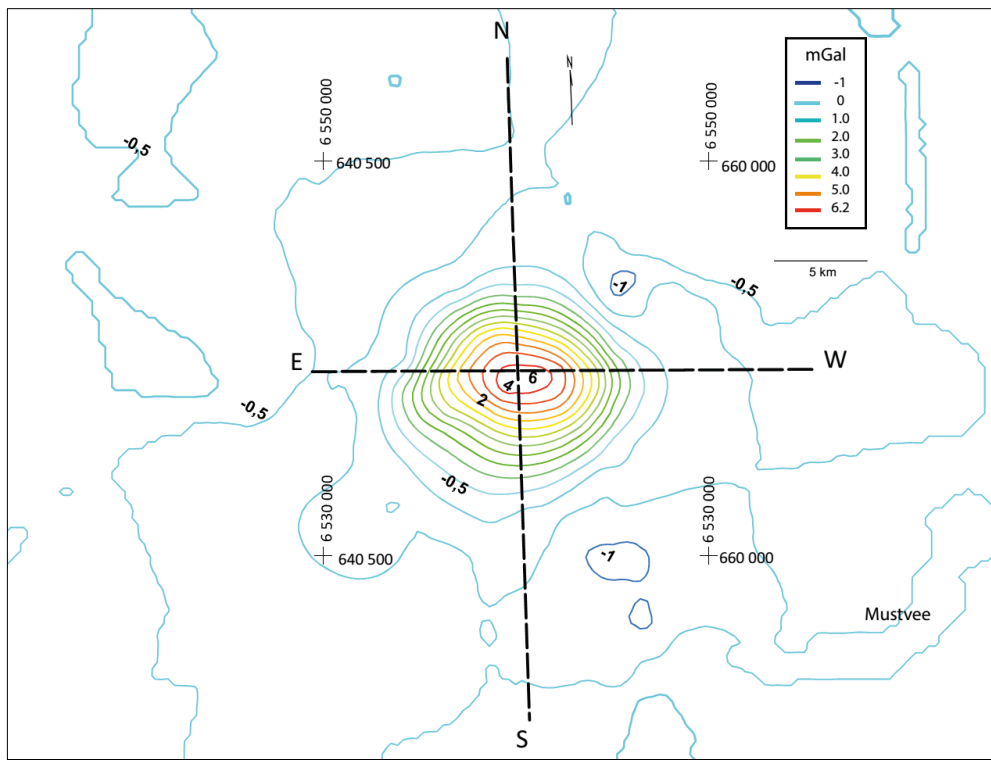


Figure 3. Bouguer anomaly contour of Luusika anomalous area. Anomaly has elliptic shape and amplitude up to 6.26 mGal.

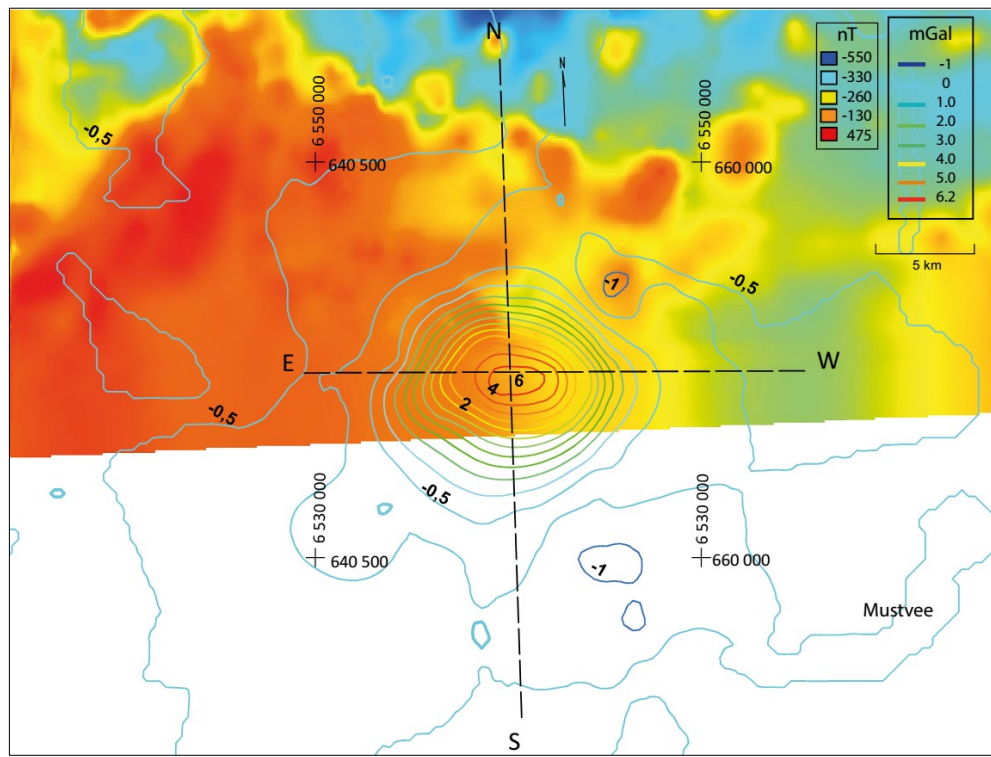


Figure 4. The Luusika Bouguer anomaly contour map on top of aeromagnetic map of northeastern Estonia. The data are from Geological Survey of Estonia and Estonian Land Board.

2. Methods and data

2.1 Ground magnetic survey

The ground measurements of magnetic field intensity in Luusika area were carried out in June and July 2014. These were done to prove or disprove the occurrence of magnetic anomaly within the gravimetrically defined anomalous area. The position and extension of profiles were chosen to extend the limits of the gravitationally anomalous area. Two (stationary and mobile) independently working time-synchronized proton precession magnetometers (G-856AX by Geometrics) were used. Stationary magnetometer was installed at the fixed position (6 541 949 N; 649 711 E; L-EST97). The Earth' magnetic field varies in intensity at a range of timescales. The base-station magnetometer was used in order to record diurnal variations at every 300 seconds (Figure 5) during the period of field-works. Magnitudes of variations were found to be as high as 50 nT, which is in perfect accordance with conclusions given e.g. in Gupta (2011).

Mobile magnetometer was carried by the two-member team equipped with hand-held GPS device. Individual measurements of the magnetic field intensity were performed at about every 100 m along 5 north-south and 2 east-west striking profiles (Figure 6), and tied with coordinates of location.

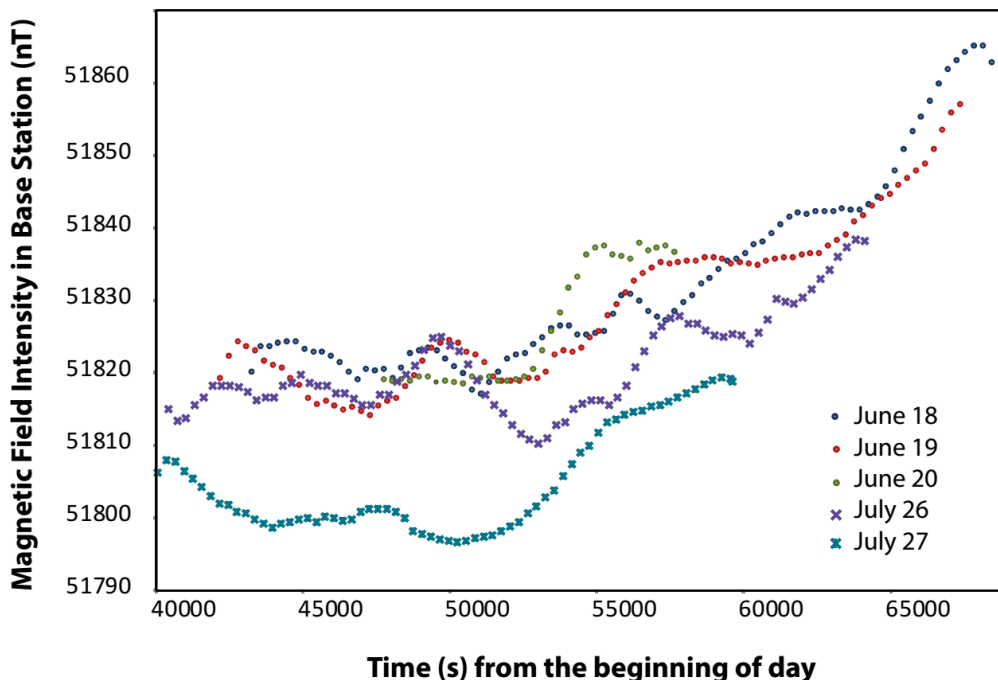


Figure 5. Diurnal changes of Earth' magnetic field in Luusika region recorded by stationary magnetometer in June and July 2014.

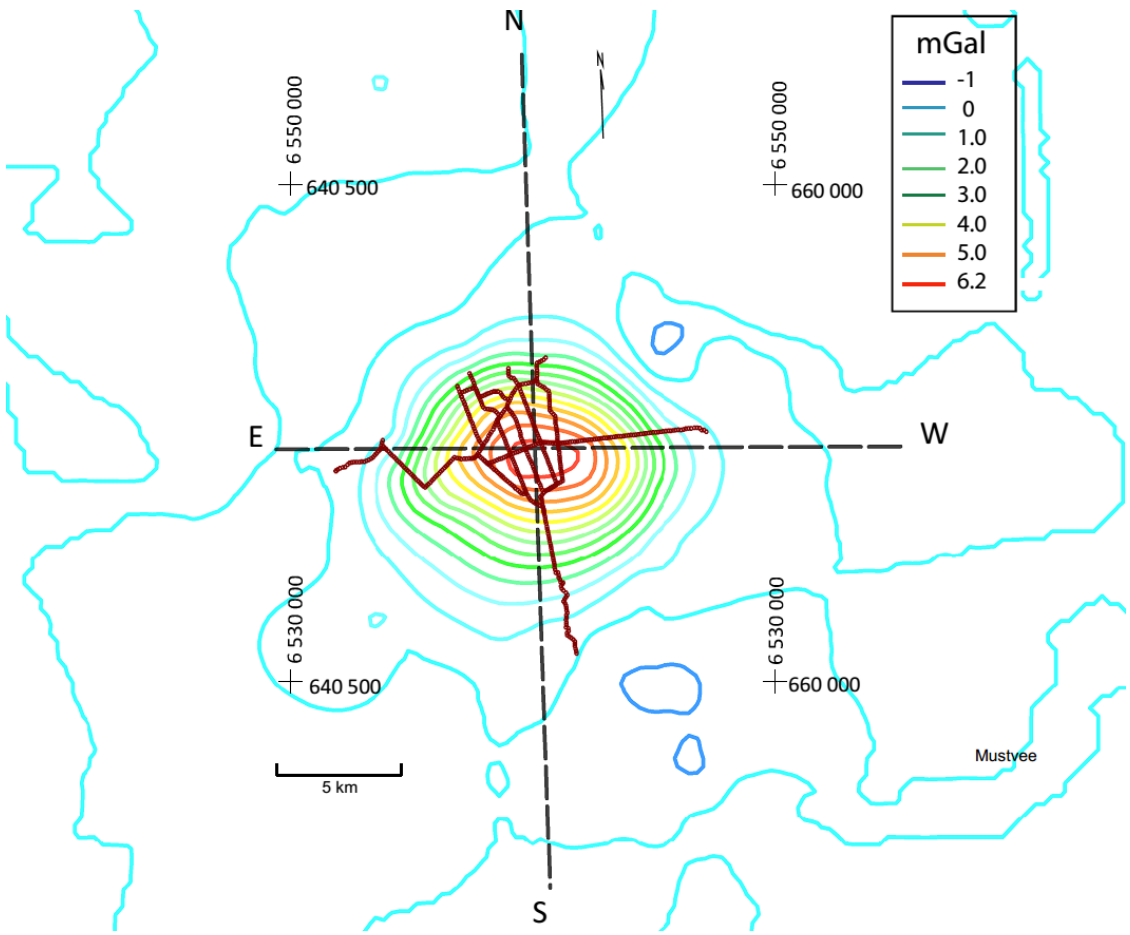


Figure 6. The ground-based magnetic survey profiles (brown) on the top of the Luusika Bouguer anomaly contour map. N-S and E-W profiles across the Bouguer anomaly have been used during depth estimation and gravity modelling. Gravity data are from Estonian Land Board.

Collected base-station readings were subtracted from the time-equivalent ground survey readings. The correction allowed obtaining a dataset without temporal variations.

2.2 Modeling

Luusika potential field anomaly is caused by an unknown source. Depth of the source and its relationships with surrounding rocks has not studied beforehand. Nevertheless, its density and magnetic susceptibility values must exceed 2680 kg/m^3 and $138 \times 10^{-6} \text{ SI}$ (background values of the Alutaguse domain), respectively, in order to produce observed positive potential field anomalies. In current work, modeling was employed in order to estimate size and physical properties of the anomaly source under study.

To reveal the deep structure and composition of the target body, Bouguer anomaly and ground-based magnetic survey datasets were plotted on the local grid coordinates (L-EST 97) in *ModelVision 14.0*. The E-W (25,450 m long) and S-N (33,525 m long) profiles across Bouguer anomaly were created. The magnetic profiles were shorter due to the insufficient amount of

ground-based data: E-W (8 400 m long) and N-S (6 800 m long); their intersection point however coincides to that of gravity profiles described above.

Direct interpretation of the gravity anomaly was conducted at first to estimate depth of the anomalous geological body. Successively, indirect interpretation (geophysical modeling) by incorporating both, gravity and magnetic data, was performed. Causative bodies of gravity and magnetic anomalies were simulated separately by models (Figure 7) whose theoretical anomalies were computed, and the shapes of the models were altered until the computed anomalies closely matched the observed anomalies.

It is however important to highlight that during the indirect interpretation of potential field data “source” is determined from the “effect”. The inverse problem has no unique solution as for a given distribution of gravity/magnetic anomaly, an infinite number of mass/magnetization distributions can be found which would produce the same anomaly.

Magnetic modelling required considering body’s apparent magnetic susceptibility (χ). Magnetic susceptibility describes magnetization response from target body placed into applied magnetic field.

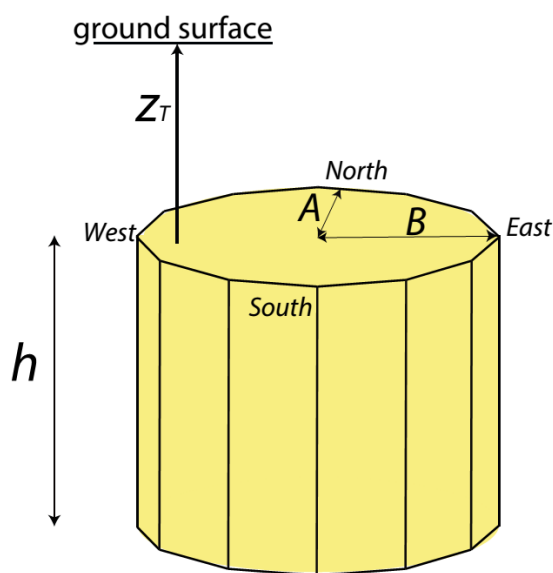


Figure 7. Modeled geological bodies were represented as elliptic pipes. Semi-axes A and B refer to body’s lateral extension in N-S and E-W directions. Parameter h characterizes vertical extension of the pipe and z_T refers to the depth to the top of the model.

Because the net magnetization is assumed to be the resultant vector of induced and remanent magnetization, Koenigsberger ratio (Q) and direction of the remanent magnetization were introduced. In the interpretation of magnetic anomalies it is important to consider both types of magnetization, because remanent magnetization can strengthen or counteract the induced magnetization (Reynolds, 2011).

Pesonen et al. (1989) compiled the palaeomagnetic poles from Fennoscandia for Early Svecofennian (1.88 Ga) and Early Subjotnian (1.6 Ga). Based on this, the earth's magnetic field position in Fennoscandia during Early Svecofennian was characterized by declination (D) of 326° and inclination (I) of 30° . Earth's magnetic field during Early Subjotnian corresponds to $D = 17^\circ$ and $I = 352^\circ$.

Table 1. Density, magnetic susceptibility, and Q-ratio of Alutaguse domain rocks [after Koppelmaa (2002) and All et al., (2004)].

Lithology	Density (kg/m ³)	Magnetic susceptibility ($\times 10^{-6}$ SI)	Q- ratio
Alutaguse domain			
migmatized gneisses	2680	138	n.d.
Pada body (gabbro and diorite)	2820	300	n.d.
mica gneiss	2690	100	n.d.
migmatite granite	2640	30	n.d.
Uljaste, Assamalla, and Haljala areas			
pyroxene gneiss, amphibole gneiss, and amphibolite	2850	3900	6.2
quartzite	2700	1700	13.9
marmor	2870	23,500	2.4
pyroxene skarn	3320	7000	22.0
migmatite granite	2630	100	6.8
Postorogenic bodies			
<i>Virtsu</i> quartz monzonite	2740	54,000	3.6
<i>Taadikvere</i> quartz monzonite	2760	38,600	0.91
Anorogenic plutons			
<i>Sigula</i> gabbro-diabase	2890	24,000	0.91
<i>Abja</i> quartz monzodiorite	2920	56,000	0.46
<i>Taebla</i> rapakivi granite	2640	1700	0.27
<i>Kloostri</i> rapakivi granite	2630	11,000	0.33
<i>Märjamaa</i> rapakivi granite I phase	2720	30,000	0.12
rapakivi granite II phase	2650	700	0.24
<i>Naissaare</i> rapakivi granite	2640	90	n.d.
<i>Neeme</i> rapakivi granite	2630	1200	0.21
<i>Ereda</i> rapakivi granite	2660	50	n.d.
<i>Riga</i> rapakivi granite	2610	2800	0.64
quartz porphyry	2620	1350	0.62
plagioclase porphyry	2810	11,800	1.04

Magnetic susceptibility background (Alutaguse Domain) was set to 138×10^{-6} SI. According to International Geomagnetic Reference Field, geomagnetic field was orientated with $I = 72.8^\circ$, $D = 8.5^\circ$ had strength (F) of 51888 nT in Luusika area at July 2014.

Each of modeled elliptic pipes was acquired physical parameters of the rocks of Alutaguse domain, post-orogenic massifs, and unorogenic plutons (given in Table 1). Their physical properties were obtained from Koppelmaa (2002), All et al. (2004), and Pesonen et al. (1989). Inverse modeling considered gravity and magnetic anomalies separately. As a result, in order to examine the inter-relation of potential field anomaly sources, the position of anomaly “source” was plotted on the magnetic and Bouguer maps.

3. Results

3.1 Depth Estimations

Interpretation of gravity data aims to examine location and depth of the causative source. At first, study was focused on the causative body depth estimation. Calculations were made along the previously described E-W and N-S profiles by half-width and gradient-amplitude ratio methods (Sharma 1976; Smith 1959; 1960). Different geometric shapes of the possible anomaly source were considered: cylinder, sphere, horizontal, and vertical cylinder, as well as tilted elliptic pipe (Table 2).

Table 2. Depth calculations of Luusika body center point by half-width and gradient amplitude method.

Geometry	Equation	Depth (m; W-E)	Depth (m; N-S)
Depth of body center point (z) by half-width method (Sharma, 1976)			
Sphere	$z = 1.035x_{1/2}$	4200	2950
Horizontal cylinder	$z = x_{1/2}$	4050	2850
Tilted elliptic pipe	$z = 0.7x_{1/2}$	2850	2000
Mean		2500	
Depth (z_T) to the top of the body (Smith 1959; 1960; Sharma 1976)			
Sphere	$z_T \leq 0.86 \frac{A_{max}}{A'_{max}}$	≤ 4100 (E side) ≤ 4900 (W side)	≤ 3000 (S side) ≤ 5400 (N side)
Horizontal cylinder	$z_T \leq 0.65 \frac{A_{max}}{A'_{max}}$	3100 (E side) 3700 (W side)	2300 (S side) 4100 (N side)
Vertical cylinder	$z_T = \frac{x_{1/2}}{\sqrt{3}}$	2350	1650
Mean		3000	

A_{max} = Bouguer anomaly maximum amplitude (Figure 8); A'_{max} = maximum horizontal gradient of the anomaly slope (Figure 9); $x_{1/2}$ = anomaly half amplitude at the half width (Figure 8); z_T = depth of top surface of model and z = depth to the body center.

Half-width method allows calculating approximate depth to the body center. The maximum amplitude (A_{max}) of Luusika's residual Bouguer anomaly reaches 6.26 mGal. Anomaly half-width values ($x_{1/2}$) at half-amplitude were measured to be 4050 m for E-W and 2850 m for N-S profile (Figure 8). According to calculations, the mean depth to the center point of the rock unit corresponds to interval of 2000 ... 4200 m (Table 2). During further gravity and magnetic modeling, the center points of elliptic pipes were placed within this interval.

Gradient-amplitude method is based on ratio between amplitude (A_{max}) and maximum gradient (A'_{max}) of the anomaly. Within the cross section two maximum horizontal gradients (A'_{max}) were measured for each side of the anomaly profile (Figure 9). The E-W profile was characterized by maximum gradients of 0.0013 mGal/m (eastern side) and 0.0011 mGal/m (western side). Analogically, the N-S cross section had maximum gradients of 0.0018 mGal/m (southern side) and 0.0010 mGal/m (northern side). The maximum depth to the top of the body was calculated for each of the geometries (Table 2). The average limiting depth to the top of the body is ~3000 m. Both of the depth calculation methods show clearly a source of the Luusika anomaly is located within the crystalline basement.

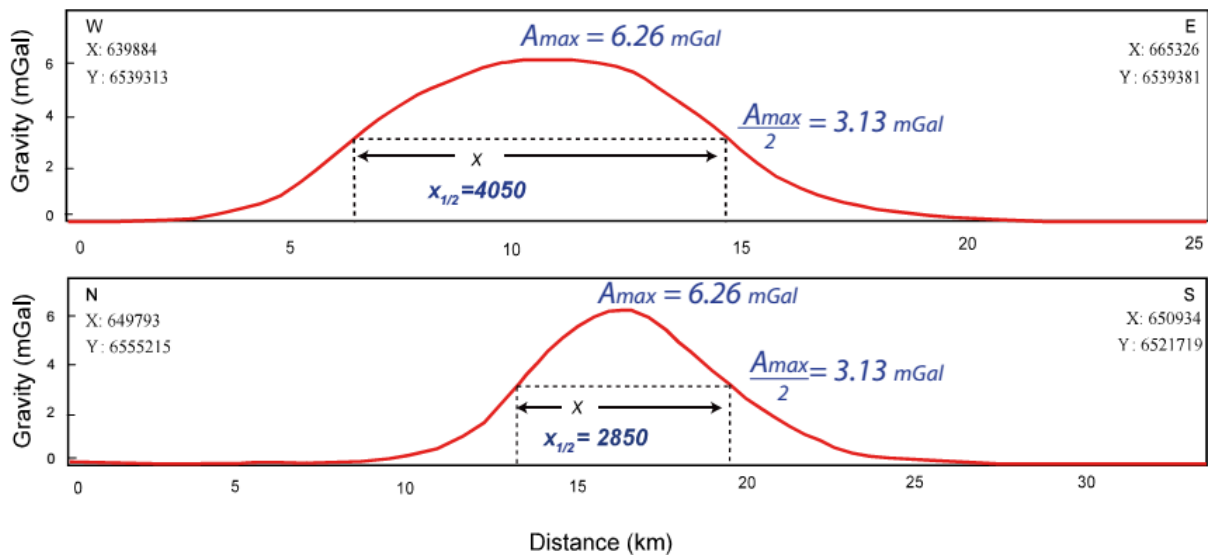


Figure 8. W-E and N-S profiles of the Luusika residual Bouguer anomaly. Anomaly width (X) is estimated at half-amplitude of 3.13 mGal. Anomaly half-width ($x_{1/2}$) was used to depth to the center of the causative body (Table 2).

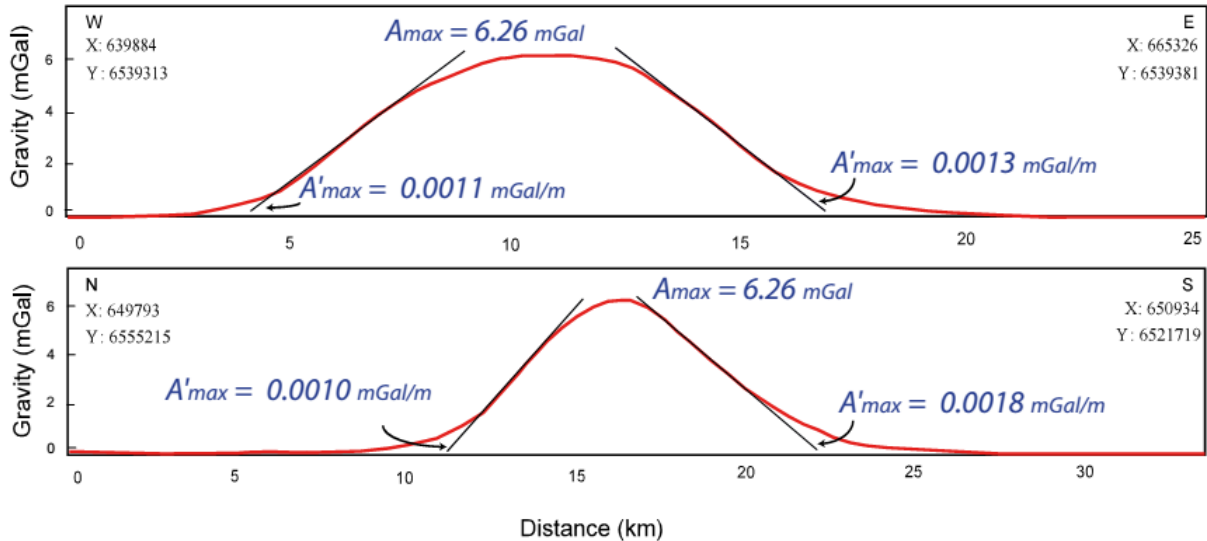


Figure 9. W-E and N-S profiles of the Luusika residual Bouguer anomaly. The slopes (A'_max) describe the steepness of the anomaly sides. The ratio between maximum amplitude and slope reflects depth of the causative body (Table 2).

3.2 Bouguer anomaly

Bouguer gravity map was visualized by minimum curvature method in *ModelVision 14.0* software. Map shows elliptic anomaly with approximate surface area of 35 km^2 . During gravity modeling two perpendicular cross sections E-W and N-S across the anomaly were employed. The gravity response of the both cross sections is characterized by a single symmetric peak with amplitude of 6.26 mGal.

Causative geological body was described as elliptic pipe and was modeled both cross sections. The body was acquired physical properties (Koppelmaa, 2002; All et al., 2004; Table 3) of various rock types in Estonian crystalline basement in order to produce calculated gravity response by trial-and-error technique. This approach presumed to change model's density until the measured and calculated curves overlap. The vertical extension of the geological body was also altered, but the center point remained between 2250 ... 3000 m.

The background density was set to 2680 kg/m^3 as average for Alutaguse rocks (after All et al., 2004). Due to superposition principle the observed gravity anomaly can however be explained by a variety of mass distributions (bodies of various compositions) at different depths (Figure 10; Table 3). In order to produce positive gravity anomaly, the causative source must have reasonable density contrast with surroundings rocks.

Densities below 2680 kg/m^3 would produce negative anomalies that contradict the observations and therefore were rejected. Densities between 2700 (Alutaguse domain

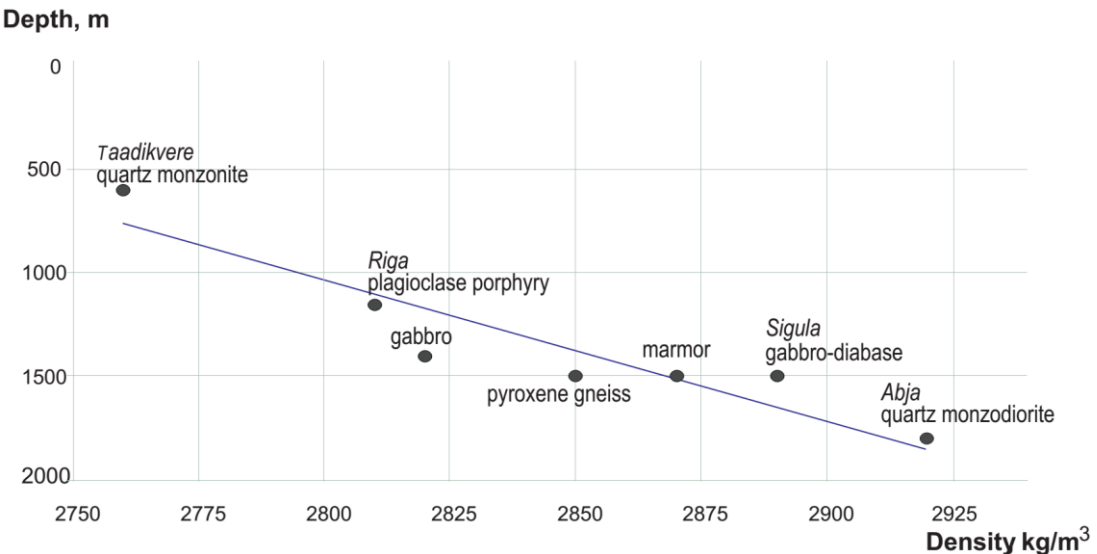


Figure 10. Relationship between density and depth to the top (z_T) of the accepted geological models (Table 3). Depth (z_T) to the top of the elliptic pipe was altered in accordance to density.

quartzite) and 2740 kg/m³ (Virtsu quartz monzonite) would need models that overlap with sedimentary cover (Appendices 5; 6; 7), and were rejected as well. The best overlap of the calculated and observed curves was achieved, when geological model had density value within the interval of 2760 ... 2920 kg/m³. Therefore, the top of elliptic pipes were placed to the depth (z_T) of 600 ... 1800 m (Figure 10; Table 3).

The top of shallowest Taadikvere-like quartz monzonite model ($\rho = 2760 \text{ kg/m}^3$) is located at 600 m (Figure 10; Table 3). Due to the relationship between elliptic pipe's density and depth, it was impossible to create geological model closer than 600 m to the surface. It indicates that Luusika body minimum density is 2740 kg/m³. The model of Abja quartz monzodiorite ($\rho = 2920 \text{ kg/m}^3$) occurred at depth of 1800 m, which is the maximum possible depth for the potential field anomaly source at given density (Figure 10; Table 3). The anomaly source placed deeper would require greater density value. As a result, the elliptic pipe acquired greater density would produce narrow-peaked calculated anomaly with steep slopes mismatching the amplitude of observed anomaly. A model (Appendix 4) of pyroxene skarn ($\rho = 3320 \text{ kg/m}^3$) was therefore rejected as well.

Altogether, seven appropriate gravity models were created and employed during further magnetic modeling. During the magnetic modeling, parameters such as depth to the top and vertical extension of elliptic pipe were not changed, but magnetic modeling required changes in horizontal dimensions and shifting the bodies laterally.

Table 3. Model (vertical pipe) properties for various rock types.

Rock type	Density (kg/m³)	z_T (m)	Dimensions (A×B×h; m)	Comment
Alutaguse domain				
Gabbro	2820	1400	1900×3900×5500	Accepted (Appendix 1)
Marmor	2870	1500	1900×4000×3000	Accepted (Appendix 2)
Pyroxene gneiss, amphibole	2850	1500	2200×4100×3000	Accepted (Appendix 3)
Pyroxene skarn	3320	2000	1500×2000×2500	Rejected (Appendix 4)
Quartzite	2700	280	2500×3000×5500	Rejected (Appendix 5)
Postorogenic plutons				
<i>Taadikvere</i> quartz monzonite	2760	600	2700×4000×5500	Accepted (Figure 12a)
<i>Virtsu</i> quartz monzonite	2740	280	3000×4500×5500	Rejected (Appendix 6)
Anorogenic plutons				
<i>Abja</i> quartz monzodiorite	2920	1800	1600×4500×3000	Accepted (Figure 13a)
<i>Sigula</i> gabbro-diabase	2890	1500	1800×3800×3000	Accepted (Figure 14a)
<i>Riga</i> plagioclase porphyry	2810	1150	2400×4100×3500	Accepted (Figure 15a)
<i>Märjamäa pluton (I phase)</i> rapakivi granite	2720	280	3000×4500×5500	Rejected (Appendix 7)

z_T = depth of top surface of model; A, B = lengths of semi-axes and h = vertical extension of the model (see Figure 7); Comment displays the result of modeling, thus “Accepted” means that model is reliable, and corresponding lithology was used for further magnetic modeling. “Rejected” models are illustrated as appendixes.

3.3 Magnetic anomaly

Magnetic anomaly map was created on the basis of ground magnetic survey. The minimum curvature method was employed for gridding data in *ModelVision 14.0* software. The map indicated the presence of magnetically anomalous area in Luusika region with maximum magnetic response of 52 215.6 nT (Figure 11) resulting from anomalously high magnetization of underlying rocks. The magnetic anomaly has elongated (in NW-SE direction) elliptic shape.

Analogically to gravity modeling, two perpendicular E-W and N-S profiles were created. E-W profile is asymmetrical; the central part is represented by plateau-like magnetic low combined with the peaks of maximum on the eastern and western side of the profile. N-S cross section is characterized by unimodal peak with asymmetrical slopes.

Geological model consisting of elliptic pipe was constructed for each of the profile. Seven residual lithologies (Table 4) were tested by trial-error technique and their shapes were altered however the vertical extension and depth to the top were equal with gravity modelling. The aim of magnetic modelling was to achieve reasonable matching of calculated and observed curves.

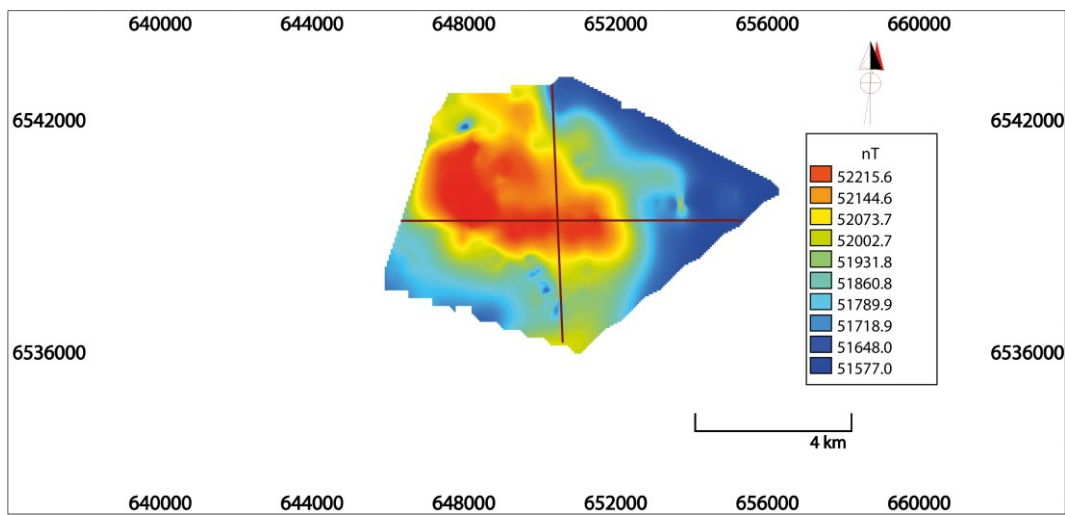


Fig. 11. Luusika area magnetic map. Profiles (brown) E-W and N-S were employed during the modelling.

Table 4. Petrophysical properties of Estonian basement rocks used during magnetic field modelling (Koppelmaa (2002) and All et al., (2004)).

Domain and Rock type							
χ ($\times 10^{-6}$ SI)	z_T	Dimensions	D	I	Q	Comment	
Meas.	Model	(m)	(A×B×h)	(m)	(°)	(°)	(-)
Alutaguse domain			Gabbro				
300	300	1500	2000×2800×5500	326	30	n.d.	Rejected Appendix 8
Marmor							
2350	2350	1500	2000×2800×3000	326	30	2.40	Rejected Appendix 9
Pyroxene gneiss							
3900	3900	1500	1700×2000×3000	326	30	6.30	Rejected Appendix 10
Postorogenic plutons			Taadikvere quartz monzonite				
38600	20000	600	1700×2500×5500	17	352	0.91	Accepted Figure 12b
Anorogenic plutons			Abja quartz monzodiorite				
56000	56000	1800	1600×2500×3000	17	352	0.46	Accepted Figure 13b
Sigula gabbro-diabase							
24000	32000	1500	1700×2000×3000	326	30	0.91	Accepted Figure 14b
Riga plagioclase porphyry							
11800	30000	1150	1800×2300×3500	17	352	1.04	Accepted Figure 15b

χ = magnetic susceptibility based on literature (Meas.; Koppelmaa, 2002; All et al., 2004) and used in models (Figures 12-15); z_T = depth of top surface of model; A, B, and h = lengths of semiaxes and vertical extension of the model (see Figure 7); D and I = declination and inclination of remanent magnetization; Q = Koenigsberger' ratio. "Accepted" models are presented as results below and discussed.

The lowest magnetic susceptibility values in Alutaguse domain lithologies range between 300 and 1800×10^{-6} SI. Calculated magnetic responses of those were too weak compared to measured data and, as a result, the models were excluded (Table 4; Appendixes 8; 9; 10). Magnetic susceptibilities of post-orogenic and anorogenic massifs are significantly higher compared to Alutaguse domain lithologies, varying between 11800 and 56000×10^{-6} SI. Modeling required occasionally stronger or weaker susceptibilities than those measured from samples (Table 4). By modifying magnetic susceptibility values, the overlap of calculated and observed data was achieved for rock types of Taadikvere, Abja, Sigula, and Riga pluton.

3.4 Geological models

Taadikvere-like model

Post-orogenic Taadikvere quartz monzonite massif has irregular round shape and diameter 8- 9 km (Koistinen, 1996). The massif was discovered geophysically and further penetrated by drill hole. Estimated U-Pb age is 1.83 Ga that however exceeds the usual age of post-orogenic rocks in Fennoscandia (Niin, 1997; Soesoo et al., 2004). On the magnetic map (Figure 1) Taadikvere body is reflected by strong circular positive anomaly.

Taadikvere massif is located within the Middle Estonian fault zone or so-called Saaremaa-Peipsi brittle shear zone. The zone is expressed as E-W striking regional linear belt of gravity and magnetic low (All et al., 2004). Drill cores originating from the Middle Estonian fault zone were characterized by cataclastites (All et al., 2004). Within or near this zone, Taadikvere and Virtsu post-orogenic quartz diorite and quartz monzonite massifs are located. It is important to highlight that estimated Luusika body is also located within the same shear zone and may represent a similar feature. The calculated gravity and magnetic responses of Taadikvere model matched the observed anomaly reasonably (Figure 12).

Taadikvere massif (SiO_2 58–62 wt%) is composed by porphyritic quartz monzonite whereas phenocrysts are represented by plagioclase. Rock contains quartz (30%), sodic plagioclase (40%), K-feldspar (15%), biotite (6%), amphibole (4%) and accessory minerals (5%) (Niin, 1997; Koppelmaa, 2002). Generally, the rock is undeformed, but gneissic structures could be observed. Density of Taadikvere body (2760 kg/m^3) allowed to model shallow geological body with top surface at the depth (z_T) of 600 m (Figure 10; Table 3).

Calculated magnetic anomaly of Taadikvere quartz monzonite model was too strong compared to observed anomaly. As a result, the magnetic model was created by incorporating lower magnetic susceptibility (20000×10^{-6} SI) than measured in Taadikvere (Table 4). Magnetic

anomaly of Taadikvere model showed negative side response at the northern side of the N-S profile (Figure 11), but in Luusika this feature is weak.

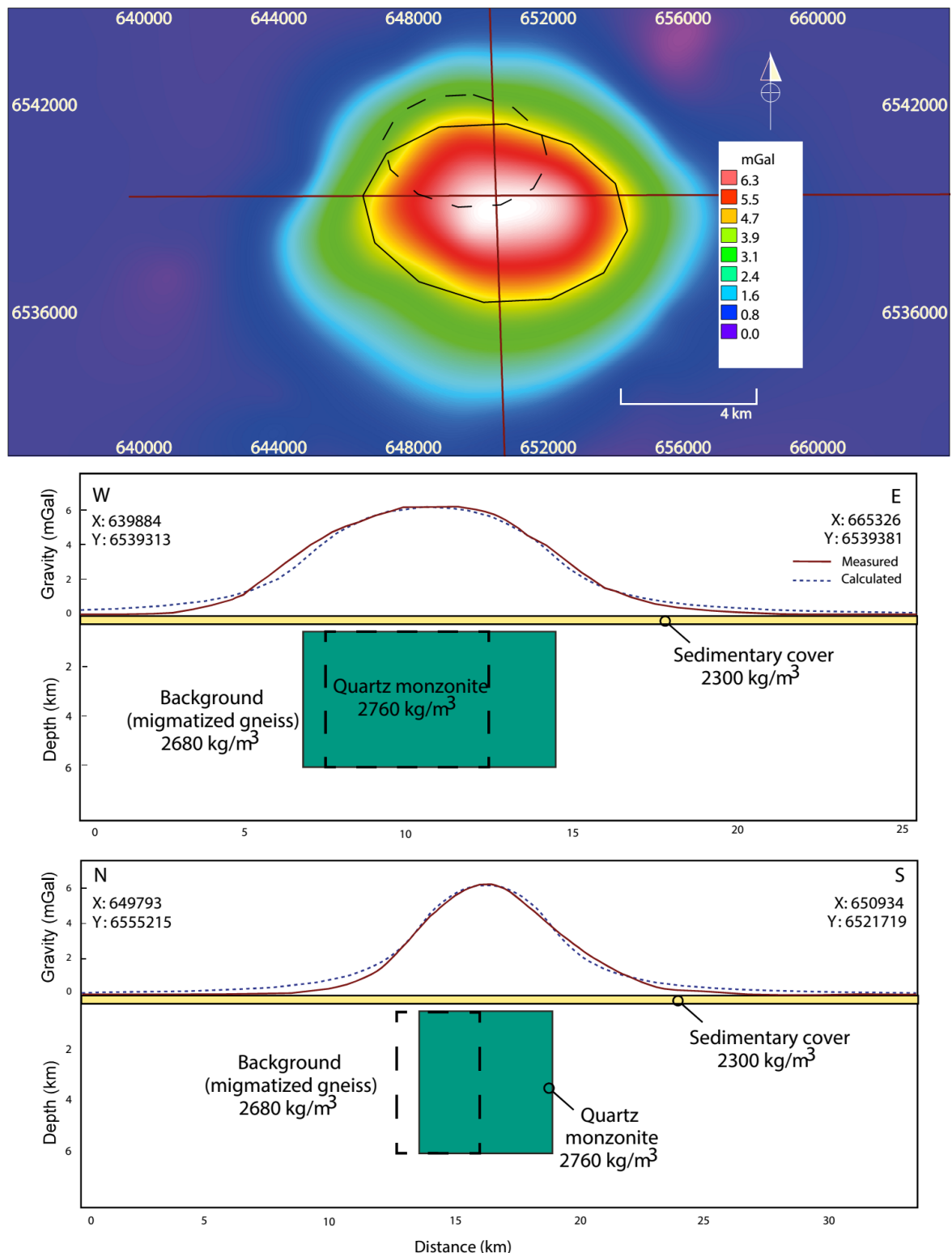


Figure 12 a. (Upper) Residual gravity anomaly over the Luusika region with outlines of gravity (solid) and magnetic (dashed) models (elliptic pipes). **Gravity profiles (middle)** and cross-sections of gravity (green rectangle) and magnetic (dashed rectangle) models along W-E (middle) and N-S (lower) profiles.

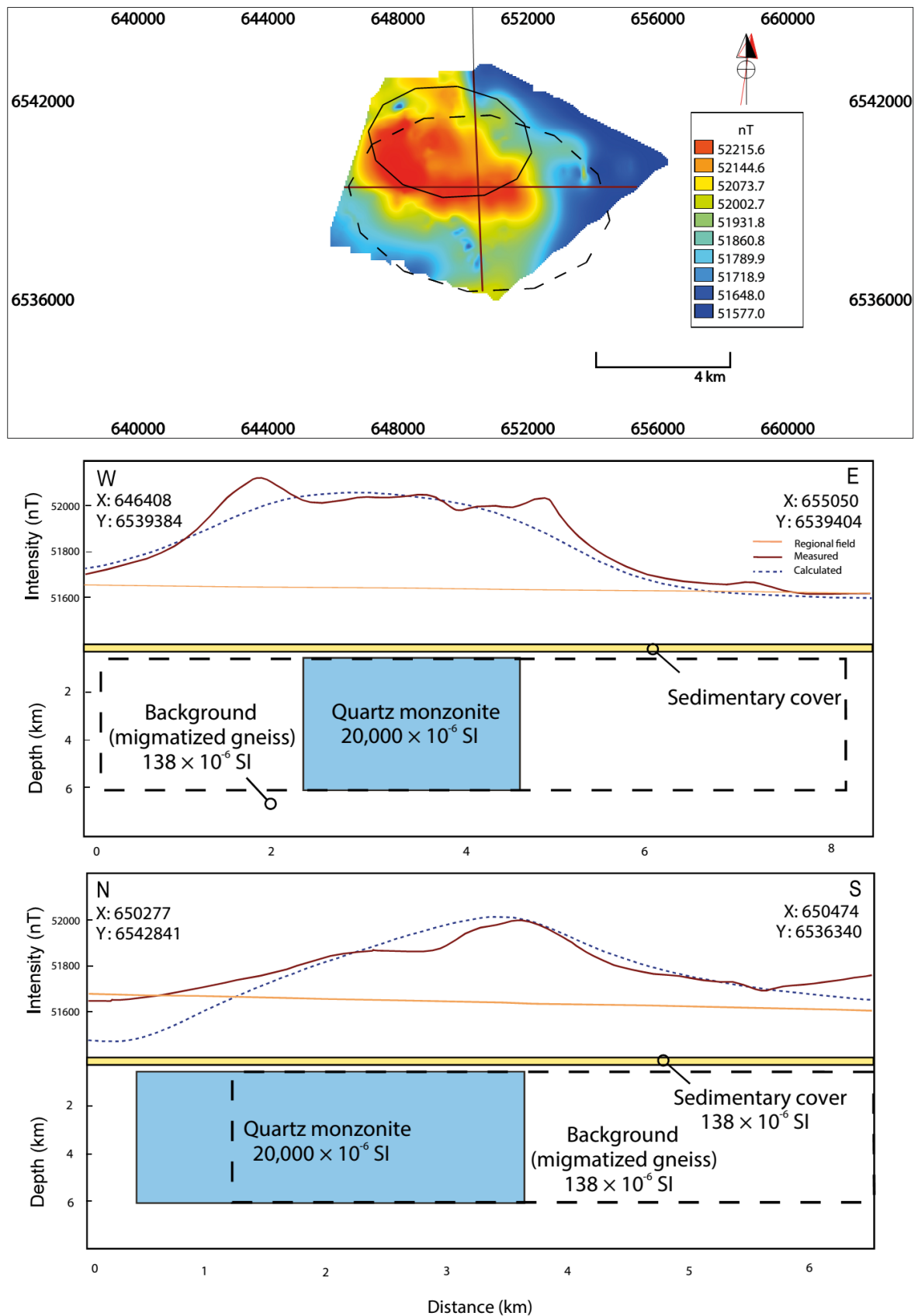


Figure 12 b. (Upper) Magnetic anomaly over the Luusika region with outlines of magnetic (solid) and gravity (dashed) models (elliptic pipes). **Magnetic profiles (measured and calculated) and cross-sections of magnetic (blue rectangle) and gravity (dashed rectangle) models along W-E (middle) and N-S (lower) profiles.**

Abja-like model

Abja massif is located within the southern Estonia domain and covered by 553 m of Paleozoic sedimentary rocks (Kirs and Petersell, 1994). The U-Pb zircon age of Abja is 1.635 ± 7 Ga (Kirs and Petersell, 1994) and that corresponds to Vyborg rapakivi province age.

The pluton was indicated by geophysical data and then opened by drill core. It occurs as elliptic body with diameter of 10 km. Abja massif (SiO_2 49 ... 54 wt%;) is characterized by strongly magnetic medium-grained quartz monzodiorite (Kirs and Petersell, 1994; Kirs et al., 2009), in places weakly gneissic and intersected by plagioclase microcline granites (Haapala and Rämö, 1991). The rock is composed by plagioclase (40 ... 50%), amphibole (10 ... 20%), biotite (10 ... 20%) and less common K-feldspar and quartz. Additionally, the rock has high concentration of accessory minerals represented by apatite (2 ... 5%) and titanomagnetite (2 ... 6%) (Koistinen, 1996).

The gravity model of Abja-like body had the highest possible density ($\rho = 2920 \text{ kg/m}^3$) that can be employed for Luusika body modelling (Table 4), which corresponded to the greatest possible depth (Figure 10). The Abja-like model has very elongated ($1.6 \times 4.5 \text{ km}$) shape. The top of elliptic pipe was placed to the depth (z_T) of 1800 m and the amplitude of calculated anomaly matched existing data (Figure 13a), however the slopes of the Bouguer anomaly profiles are slightly steeper.

The measured apparent magnetic susceptibility of Abja quartz monzodiorite is the highest amongst the post-orogenic and anorogenic intrusions ($\chi = 56000 \times 10^{-6} \text{ SI}$) due to the high content of magnetic minerals (Kirs and Petersell, 1994; Koistinen, 1996; Koppelmaa, 2002). As a result, Abja-like magnetic model was only one created by incorporating the measured magnetic susceptibility (Table 4; Figure 13b), the calculated magnetic response was however slightly weaker than Luusika magnetic anomaly (Figure 13b).

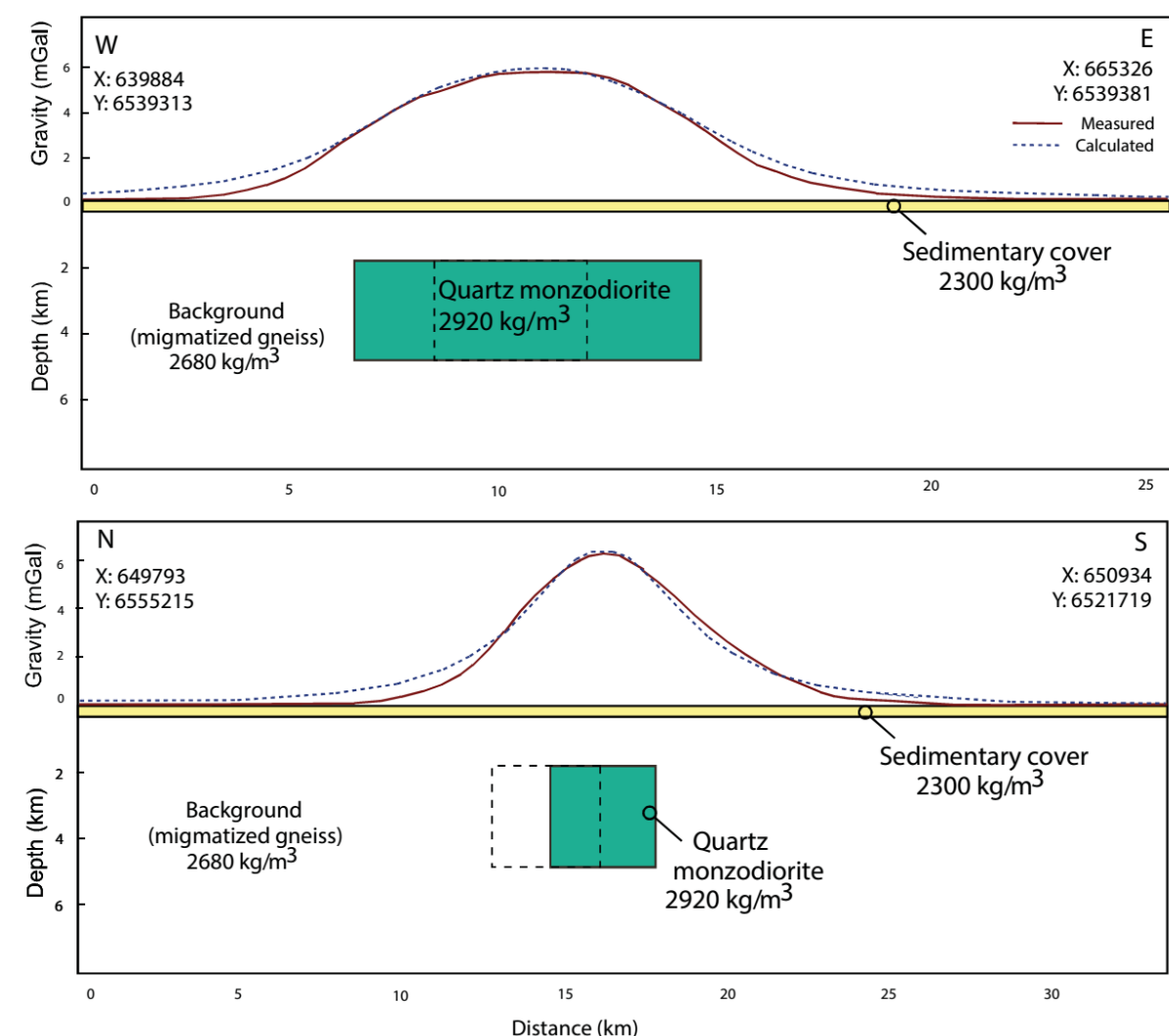
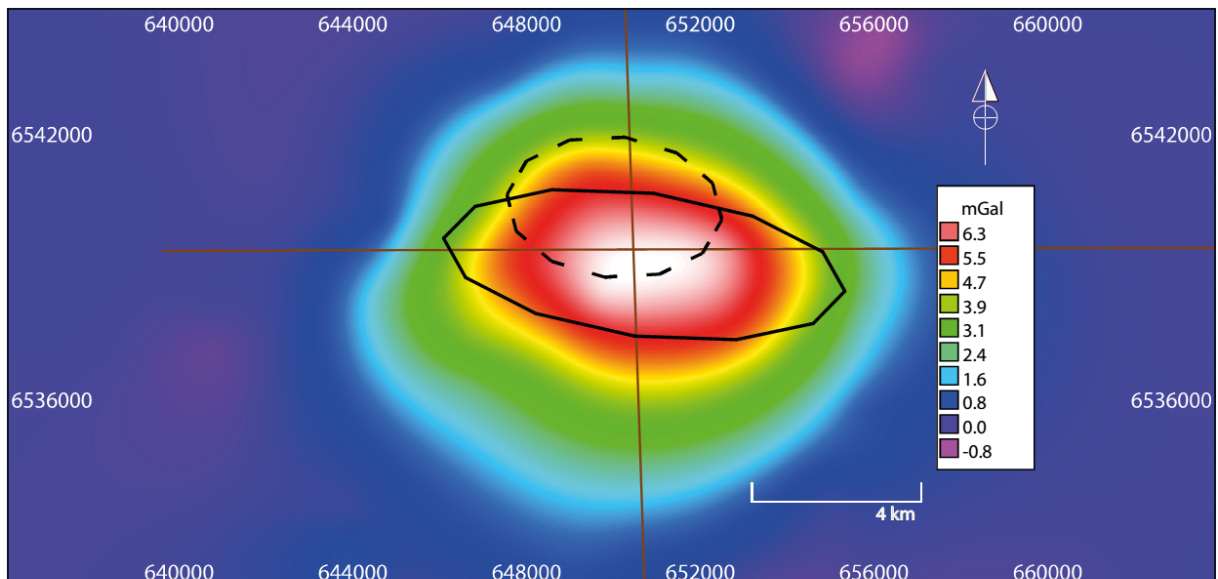


Figure 13 a. (Upper) Residual gravity anomaly over the Luusika region with outlines of gravity (solid) and magnetic (dashed) models (elliptic pipes). Gravity profiles (measured and calculated) and cross-sections of gravity (green rectangle) and magnetic (dashed rectangle) models along W-E (middle) and N-S (lower) profiles.

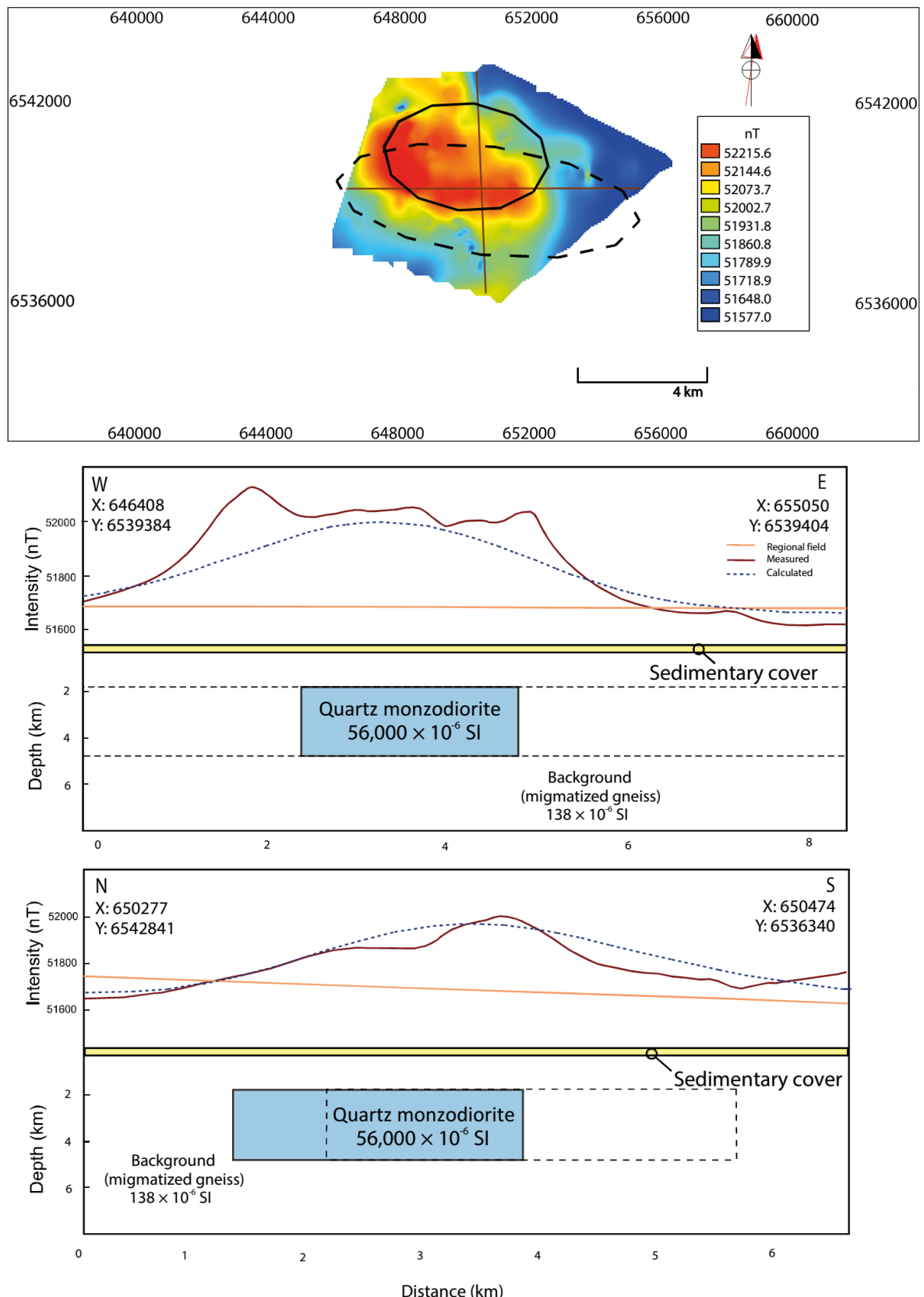


Figure 13 b. (Upper) Magnetic anomaly over the Luusika region with outlines of magnetic (solid) and gravity (dashed) models (elliptic pipes). **Magnetic profiles (measured and calculated) and cross-sections of magnetic (blue rectangle) and gravity (dashed rectangle) models along W-E (middle) and N-S (lower) profiles.**

Sigula-like model

Sigula is N-E trending magmatic body with dyke-like geometry: 1.5 km long and 4 km wide (Haapala and Rämo, 1991; Koppelmaa, 2002). Massif lies within the eastern part of Tallinn domain (Figure 1) in the deep Proterozoic fault zone of NE-SW direction (Koppelmaa and Kivisilla, 1998); it is covered by 180 m of Palaeozoic rocks. The rock of Sigula has phaneritic texture, it is composed by ophitic gabbro-diabase (SiO_2 47 ... 49 %) with high content of accessory minerals: apatite 3 ... 6 % and ore minerals (titanomagnetite, magnetite and less common sphalerite, galena, and molybdenite) 6 ... 10 % (Koppelmaa, 2002; Koppelmaa and Kivisilla, 1998).

The estimated K-Ar age of biotite originating from Sigula diabase is 1.686 Ga (Koppelmaa and Kivisilla, 1998), which corresponds to the Vyborg rapakivi suite. The Vyborg batholith consists of numerous intrusive felsic phases and mafic rocks. The scattered gabbroidic and anorthositic inclusions up to 1-2 km in diameter have been documented, however they are very minor by volume (Koistinen, 1996). The gabbro-diabase of Sigula represents mafic magmatism in Estonian basement, it is located amongst the local assemblage of rapakivi (Naissaare, Ereda, Märjamaa, Neeme), but its relation any of them is unknown. The geochemical comparison of Sigula rock with mafic rapakivi related Breven-Hällerforsi dolerite dykes revealed similarities; in addition, the unmethamorphosed expression of gabbro-diabase also suggests that Sigula belongs to the Vyborg rapakivi related satellite group (Kolbak, 2011).

Sigula massif ($\rho = 2890 \text{ kg/m}^3$) is composed by denser rocks than Taadikvere quartz monzonite described above. The density contrast with hosting Alutaguse mica gneisses is 210 kg/m^3 . As a result, elliptic pipe was modelled at greater depth of 1500 m compared to Taadikvere-like model (Figure 10).

Sigula diabase is also characterized by high magnetic susceptibility due to the remarkable apatite-magnetite mineralization (Koppelmaa and Kivisilla, 1998). Magnetic susceptibility varies within the rock, therefore, Koppelmaa (2002) documented apparent magnetic susceptibility in Sigula $\chi = 24000 \times 10^{-6}$ SI, however, Koppelmaa and Kivisilla (1998) documented the value of $\chi = 32000 \times 10^{-6}$ SI. Response of magnetic model of Sigula-like body matched smoothly discovered Luusika anomaly when magnetic susceptibility was set to $\chi = 30000 \times 10^{-6}$ SI (Table 4).

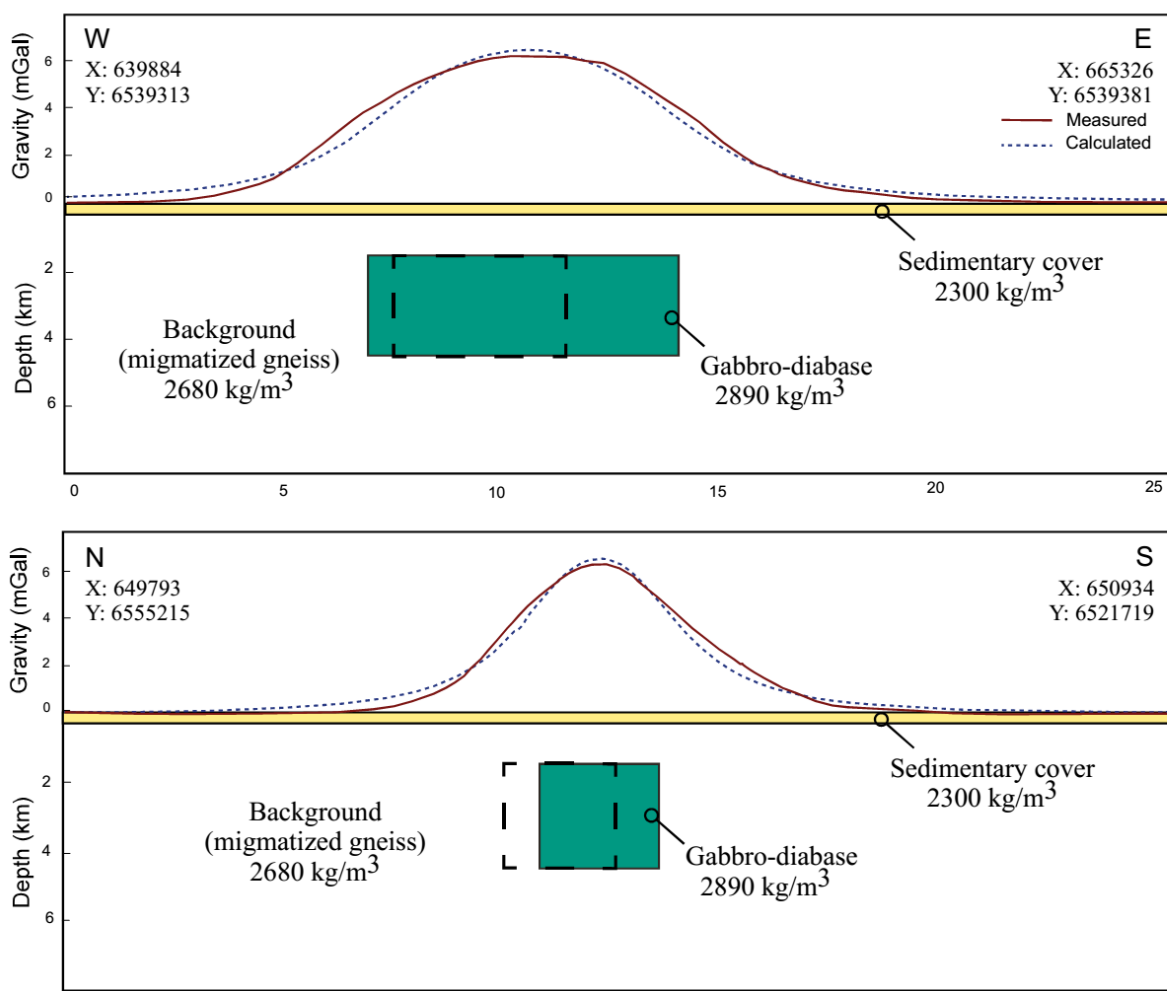
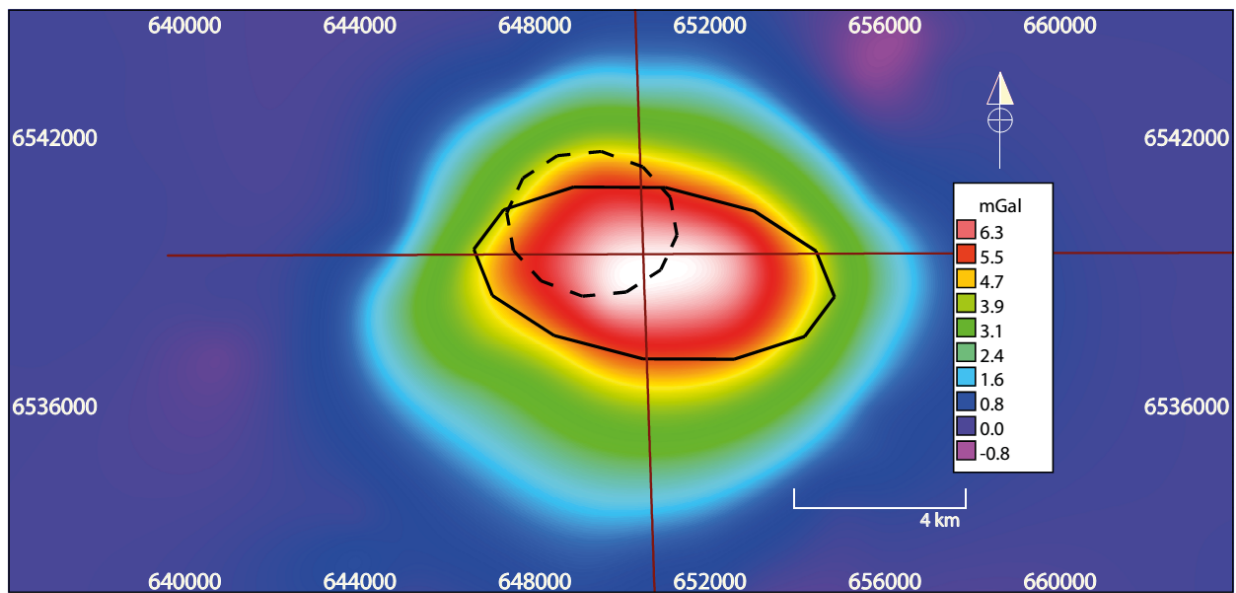


Figure 14 a. (Upper) Residual gravity anomaly over the Luusika region with outlines of gravity (solid) and magnetic (dashed) models (elliptic pipes). Gravity profiles (measured and calculated) and cross-sections of gravity (green rectangle) and magnetic (dashed rectangle) models along W-E (middle) and N-S (lower) profiles.

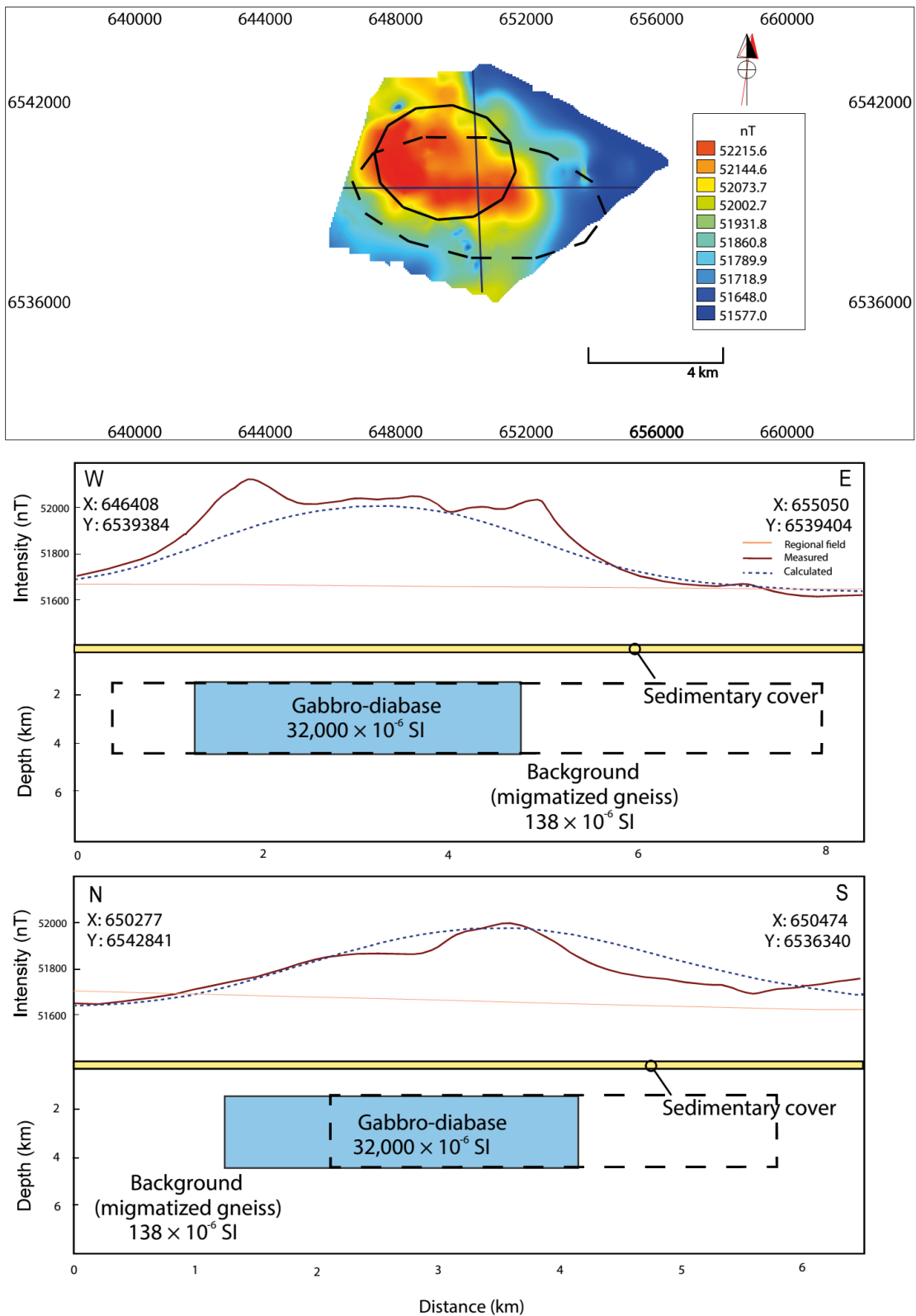


Figure 14 b. (Upper) Magnetic anomaly over the Luusika region with outlines of magnetic (solid) and gravity (dashed) models (elliptic pipes). Magnetic profiles (measured and calculated) and cross-sections of magnetic (blue rectangle) and gravity (dashed rectangle) models along W-E (middle) and N-S (lower) profiles.

Riga plagioclase porphyry-like model

Riga pluton belongs to slightly younger Riga-Åland rapakivi province 1.59 ... 1.54 Ga. The rocks of Riga batholith are very varying. Northern part of the pluton is characterized by “typical” felsic rapakivi granites. The southern and central part is represented by wide range of intermediate and basic rocks (Koistinen, 1996; Koppelmaa, 2002). During the modeling, the physical properties of plagioclase porphyry originating from Riga province were considered. The matrix is composed by plagioclase (65 ... 75 %), pyroxene (15 ... 25 %), minor amphibole, biotite and accessory minerals. Idiomorphic plagioclase phenocrysts represent 3 ... 10 % of the rock (Puura et al., 1983; Koppelmaa, 2002).

During gravity modeling, the elliptic pipe simulating plagioclase porphyry ($\rho = 2810 \text{ kg/m}^3$) was placed at the top depth (z_T) of 1150 m. Simulated magnetic model was acquired higher magnetic susceptibility ($\chi = 30000 \times 10^{-6} \text{ SI}$) value than measured (Table 4), and slight discrepancy between observed magnetic anomaly and calculated response might be observed at the northern side of N-S cross section (Figure 15b). The simulated gravity and magnetic anomalies of plagioclase porphyry matched existing data (Figure 15). Apparently, the characteristics of Riga plagioclase porphyry fall in the range of petrophysical properties estimated for Luusika rock unit.

The distribution of Riga-Åland rapakivi related rocks is limited to the southeastern Finland and northeastern Latvia (Puura and Flodén, 2000). Due to the age-and-space relationship of rapakivi rocks, it is unlikely that Luusika body belongs to the Riga-Åland rapakivi province and as a result, the model was rejected despite the petrophysical similarities and “matched” gravity and magnetic responses.

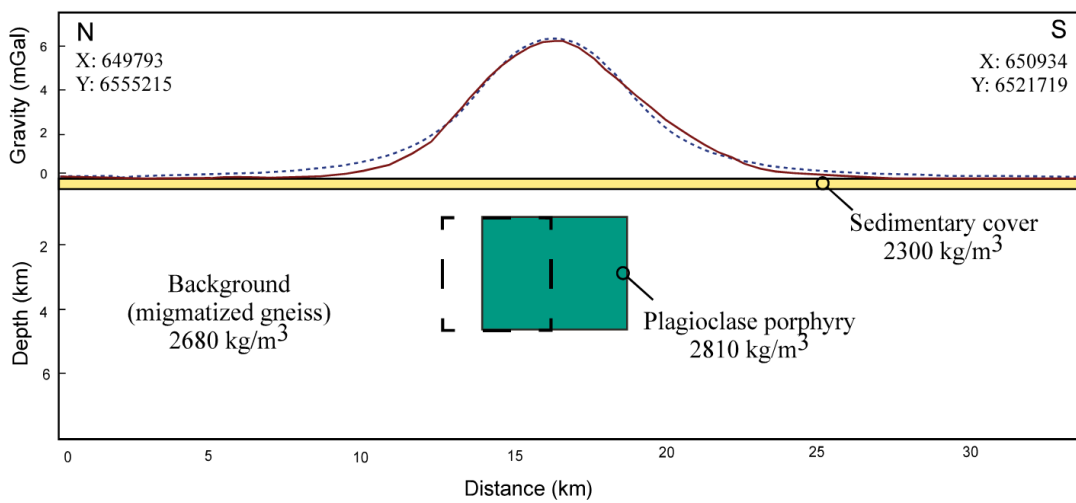
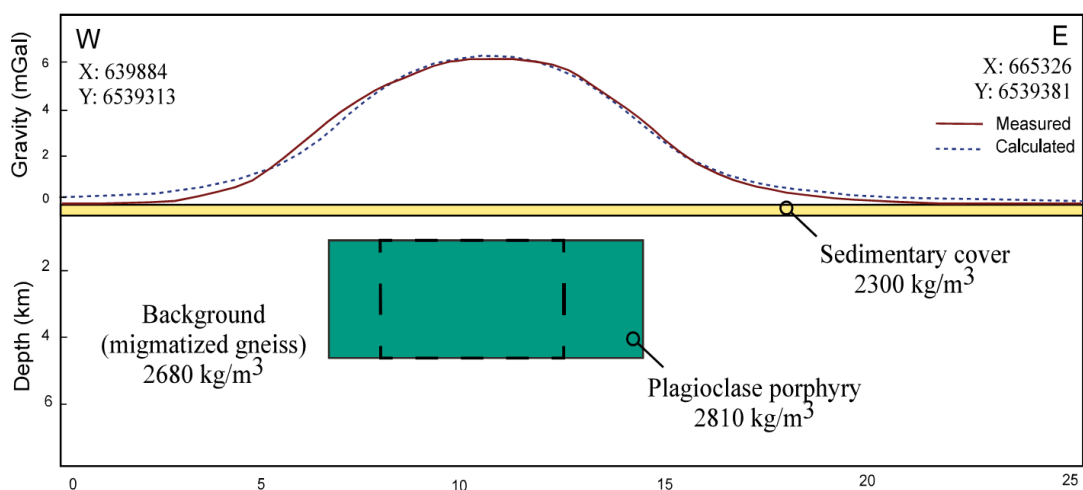
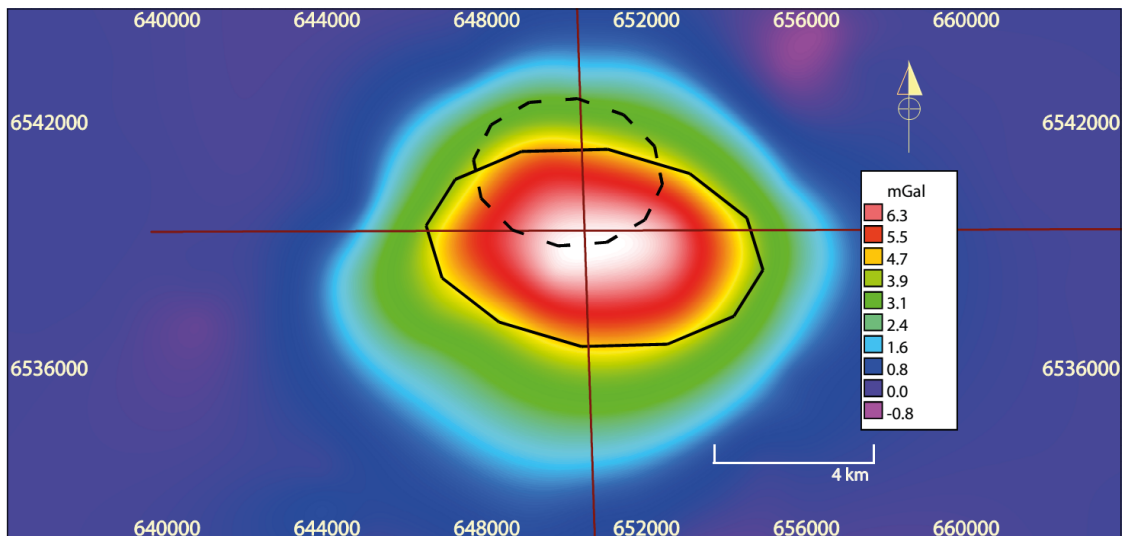


Figure 15 a. (Upper) Residual gravity anomaly over the Luusika region with outlines of gravity (solid) and magnetic (dashed) models (elliptic pipes). Gravity profiles (measured and calculated) and cross-sections of gravity (green rectangle) and magnetic (dashed rectangle) models along W-E (middle) and N-S (lower) profiles.

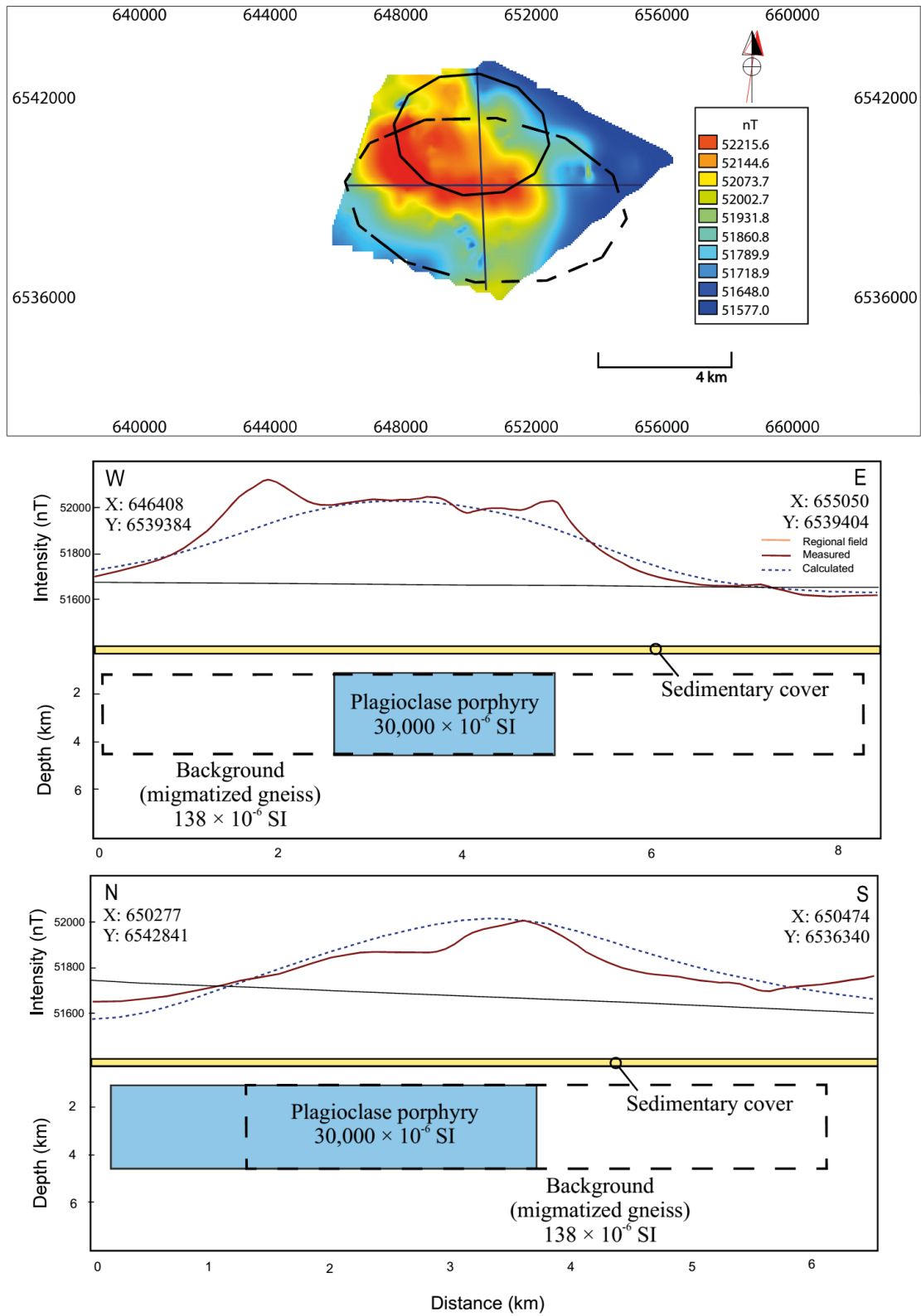


Figure 15 b. (Upper) Magnetic anomaly over the Luusika region with outlines of magnetic (solid) and gravity (dashed) models (elliptic pipes). **Magnetic profiles (measured and calculated) and cross-sections of magnetic (blue rectangle) and gravity (dashed rectangle) models along W-E (middle) and N-S (lower) profiles.**

4 Discussion

The gravity and magnetic anomalies are results of physical parameters such as density and magnetization in respect to surrounding properties, and location and volume of the anomalous unit. In Luusika, Bouguer and ground-based magnetic field data showed positive anomalies clearly associating with denser and more magnetic anomalous rock unit compared to Alutaguse mica gneisses. The gravity and magnetic anomalies are partly overlapping, hinting that Luusika feature is not homogenous and denser masses are necessarily not more magnetic. This is a reason why modeling of gravity and magnetic fields by identical body failed. In all the models, the magnetic anomaly and its geological source are smaller and located north to north-west from a center of gravity anomaly (Figures 12-15).

Several igneous rock types were proposed to be the causative source. According to modeling results and geological/geochronological studies of Estonian basement, Luusika body belongs to **i)** Svecofennian post-orogenic rock group or **ii)** anorogenic Vyborg rapakivi suite. As a result, derived models simulated rock types of post-orogenic Taadikvere and anorogenic Abja and Sigula massifs.

Gravity modelling revealed that Luusika feature top (z_T) lies between 600 and 1800 m below ground surface. At given top depth, the anomaly source must have density values in a range of 2760 ... 2920 kg/m³. That interval corresponds to densities of intrusions occurring in Estonian basement varying from intermediate to mafic in composition.

Out of all simulated rock types, Taadikvere quartz monzonitic intrusion is the closest to Luusika area (Figure 1). The E-W striking Middle-Estonian fault zone hosts the documented Muhu, Virtsu (3 ... 4 km in size) and Taadikvere (7 ... 8 km in size) post-orogenic quartz monzonitic and granodioritic granitoids, which appeared in a brittle crust environment predating the rapakivi event (Puura and Flodén, 2000). Intrusions are contoured by elliptic or circular magnetic anomalies explained by anomalously high content of ore and accessory minerals (Niin, 1996). It is important to highlight, that intrusions are related to the deep Middle-Estonian fault zone.

The geometry of Luusika Bouguer anomaly also refers to the undeformed circular or elliptic body with E-W lateral extension of ~8 km (Figure 13a) similar to Taadikvere. The lateral extension of magnetic anomaly source is somewhat less being ~5 km (Figure 13b).

According to magnetic modelling, Luusika rock unit has magnetic susceptibility interval of $\bar{\chi} = 20\ 000 \dots 56\ 000 \times 10^{-6}$ SI. The measured magnetic susceptibilities of post-orogenic

Taadikvere ($\bar{\chi} = 38\ 600 \times 10^{-6}$ SI) and Virtsu ($\bar{\chi} = 54\ 000 \times 10^{-6}$ SI) massifs are falling to this range, supporting the post-orogenic origin of Luusika feature.

On the other hand, unorogenic intrusions are the same way candidates for Luusika potential field anomalies source. Sigula fault related dyke-like gabbro-diabase is located in Tallinn domain and ellipse-shaped Abja quartz monzodiorite lies within southern Estonia granulite domain (Figure 1). Both intrusions are mafic (SiO_2 47 ... 52 wt%) and have the highest densities amongst the all simulated rock types (Table 3; Figure 10). According to Petersell et al (1985), intrusions are also characterized by gravity anomaly of 1.5 mGal (Sigula) and 2.5 mGal (Abja). Sigula diabase intrusion also appears as local positive anomaly on the magnetic map (Koppelmaa and Kivisilla, 1998). Abja ($\bar{\chi} = 56000 \times 10^{-6}$ SI) and Sigula ($\bar{\chi} = 24000 \times 10^{-6}$ SI) have considerable higher magnetic susceptibilities compared to the hosting Alutaguse domain, as a result, both models produced “matching” models.

As it has been introduced above, the aeromagnetic map (1: 25 000) did not revealed magnetic anomaly in studied region. In order to get better understanding of Luusika anomaly and possible similar anomalies within Middle Estonia fault zone, additional magnetic survey must be carried out. Despite this, the geophysical approach is not always sufficient for mapping the deep structures of Estonian Precambrian rocks. Previous geophysical studies of Estonian basement were supported by drill holes and rocks were dated and compared geochemically with similar material in Sweden and Finland. This approach resulted in precise regional maps and better understanding of Svecofennian orogeny and following magmatic events.

Apparently, modeling allowed eliminating rock units that cannot be the causative sources of potential field anomaly under study, and estimate the ranges of Luusika body petrophysical properties. For additional understanding of the Luusika feature, deep drilling is required.

5. Conclusion

The high positive gravity anomaly values discovered by Estonian Land Board in 2010-2011 indicated gravity increase of 6.3 mGal in Luusika area. The ground-based magnetic survey identified magnetic anomaly within Luusika area and gave new information of the underlying rock unit magnetic properties. The ground-based magnetic measurements showed good correlation to the observed Bouguer anomaly.

The depth estimation was done on the basis of Bouguer anomaly profiles. The calculations suggested that Luusika rock unit does likely not outcrop under sedimentary cover. The mean anomaly-mass center point (z) was estimated to be 2500 m whereas the calculated result of maximum limiting depth (z_T) of the body top is 3000 m.

The data were sufficient for creating models of causative source and testing different lithologies. For magnetic modeling the orientation of remanent magnetization was necessary to produce reliable model. Remanent magnetization was characterized by age-appropriate direction. The lithologies of Alutaguse domain and post-orogenic and anorogenic intrusions were simulated. Conclusions of the modelling are:

1. The depth (z_T) to the top of the body is 600 ... 1800 m.
2. The density of Luusika Bouguer anomaly causative source is 2760 ... 2920 kg/m³.
3. Magnetic anomaly is produced by rock unit with very high magnetic susceptibility values of $\bar{\chi} = 20000 \dots 56000 \times 10^{-6}$ SI compared to the background.

Similar petrophysical properties are documented for post-orogenic and anorogenic plutons occurring in Estonian basement. The Luusika anomaly lies within the Middle-Estonia fault zone, which hosts several post-orogenic intrusions; as a result, it could be interpreted as Taadikvere-like rock unit. Also, a few rapakivi related intrusions (Abja and Sigula) discovered in Precambrian basement of Estonia could be proposed to be the source of the potential field anomalies.

The modeling and comparison of petrophysical properties of lithologies suggest that Luusika causative source is intermediate to mafic rock by composition, similar to Abja, Sigula, or Taadikvere and probably related to presence of Middle-Estonian fault zone.

Acknowledgments

There have been a lot of people contributing to this work. I would like to thank all students involved to the Geophysical Exploration field training and supervisors Jüri Plado and Argo Jõeleht for assistance and all the hard work.

Special regards to Tõnis Oja, chief specialist at Estonian Land Board for taking the role of supervisor and providing the data. I would like to thank Juho Kirs for very interesting discussions that helped throughout the work. I express my sincere appreciation to my family and friends and to all who also helped me directly or indirectly.

I would like to express my greatest appreciation to Jüri Plado for his patient support and uncountable hours of assistance.

References

- All, T., 1995, Lokaalsete magnetiliste anomaliate paiknemise seaduspärasustest ja geoloogilis-geofüüsikalisest tõlgindamisest Eestis (in Estonian), MSc thesis, University of Tartu, 96 p.
- All, T., Puura, V. and Vaher, R., 2004, Orogenic structures of the Precambrian basement of Estonia as revealed from the integrated modelling of the crust, *Proceedings of the Estonian Academy of Sciences*, vol. 53 Issue 3, p. 165-189.
- Bloom, A. and Oja, T., 2010, Raskuskiirenduse mõõdistamised Pärnu, Lääne-Viru, Jõgeva ja Põlva maakondades (in Estonian), Fieldwork report, 70 p.
- Bogdanova, S.V., Bingen, B., Gorbatschev, R., Kheraskovac, T. N., Kozlov, V. I., Puchkov, V. N. and Volozh, Yu. A, 2008, The East European Craton (Baltica) before and during the assembly of Rodinia, *Precambrian Research*, vol. 160, p. 23-45.
- Bogdanova, S., Gorbachev, R., Skridlaite, G., Soesoo, A., Taran, L. and Kurlovich, D., 2015, Trans-Baltic Palaeoproterozoic correlations towards the reconstruction of supercontinent Columbia/Nuna, *Precambrian Research*, vol. 259, p. 5-33.
- Gupta, H. K. 2011, The Encyclopedia of Solid Earth Geophysics, Springer, The Netherlands, 1539 p.
- Haapala, I. and Rämö, T., (editors) 1991, Symposium on rapakivi granites and related rocks Abstract volume, Guide 34, Geological Survey of Finland, 65 p.
- Haapala, I., Rämö, T. and Frindt, S., 2005 Comparision of Proterozoic and Phanerozoic rift-related basaltic granitic magmatism, *Lithos*, vol. 80, p. 1-32.
- Kirs, J. and Petersell, V., 1994, Age and geochemical character of plagiomicrocline granite veins in the Abja gabbro-dioritic massif, *Tartu Ülikooli toimetised*, vol. 972, p. 3-15.
- Kirs, J., Puura, V., Soesoo, A., Klein, V., Konsa, M., Koppelmaa, H., Niin, M. and Urtson, K., 2009, The crystalline basement of Estonia: rock complexes of the Palaeoproterozoic Orosirian and Statherian and Mesoproterozoic Calymian periods, and regional correlations, *Estonian Journal of Earth Science*, vol. 58, p. 219-228.
- Kolbak, E, 2011, Petrographical and geochemical characteristics of mafic Sigula massif, MSc thesis, University of Tartu, 54 p.

Koistinen, T. (editor), 1996, *Explanation to the Map of Precambrian basement of the Gulf of Finland and surrounding area 1:1 million*, Geological Survey of Finland, Espoo, 141 p.

Koppelmaa, H., 2002, Geological map of the crystalline basement of Estonia Scale 1:400000 Explanation to the map Estonian version, Geological Survey of Estonia, 32 p.

Koppelmaa, H. and Kivililla, J., 1998, Geological map of the crystalline basement of Northern Estonia. Scale 1 : 200 000. Explanation to the map. Geological Survey of Estonia, 33 p., 15 tables, 1 plate of photos, 4 appended maps.

Lahtinen, R., Garde, A. A. and Melezhik, V. A., 2008, Paleoproterozoic evolution of Fennoscandia and Greenland, *Episodes*, vol. 31, No. 1, p. 20-28.

Niin, M, 1996, Svecofennian granitoids of Estonian crystalline basement (in Estonian), MSc thesis, University of Tartu, 31 p.

Niin, M, 1997, Svecofennian granitoids of the crystalline basement of Estonia; classification on the basis of geological structure, mineral and chemical composition. Bulletin of the Geological Survey of Estonia vol. 7, p. 4-3.

Nironen, M., 1997, The Svecofennian Orogen: a tectonic model, *Precambrian research*, vol. 86, p. 21-44.

Oja, T., 2011, Raskuskiirenduse anomaalvälja kerkest Luusika kandis ning selle mõjust geoidile (in Estonian), *Geodeet*, vol. 41(65), p. 26-30.

Pesonen, L. J., Torsvik, T. H., Elming S.-A. and Bylund, G., 1989, Crustal evolution of Fennoscandia – palaeomagnetic constrains, *Tectonophysics*, vol. 162, p. 27-49.

Petersell, V., Talpas, A. and Põldvere, A., 1985, Otchet ob izuchenii zelezorudnyh formatsii v dokembrii Estonii (in Russian), Tallinn, EGF.

Puura, V. and Flodén, T., 1999, Rapakivi-granite–anorthosite magmatism — a way of thinning and stabilisation of the Svecofennian crust, Baltic Sea Basin, *Tectonophysics*, vol. 305, p. 75-92.

Puura, V. and Flodén, T., 2000, Rapakivi-related basement structures in the Baltic Sea area; a regional approach, *GFF*, vol. 122, p. 257-272.

Puura, V., Klein, V., Koppelmaa, H. and Niin, M., 1997, III Precambrian Basement, *Geology and mineral resources of Estonia*, Tallinn, p. 27-34.

Puura, V., Vaher, R., Klein, V., Koppelmaa, H., Niin, M., Vanamb, V. and Kirs, J., 1983, *The Crystalline Basement of Estonian Territory*, Nauka, Moscow (in Russian, with extended English summary), 207 p.

Reynolds, J. M., 2011, An introduction to Applied and Environmental Geophysics, 2nd edition, Wiley-Blackwell, p 710.

Sharma, P.V., 1976. *Geophysical Methods in Geology*. Elsevier, Amsterdam, 428 p.

Smith, R.A., 1959. Some depth formulae for local magnetic and gravity anomalies. *Geophysical Prospecting*, vol. 7, p. 55-63.

Smith, R.A., 1960. Some formulae for interpreting local gravity anomalies. *Geophysical Prospecting*, vol. 8, p. 607-613.

Soesoo, A., Puura, V., Kirs, J., Petersell, V., Niin, M. and All, T., 2004, Outlines of the Precambrian basement of Estonia, *Proceedings of the Estonian Academy of Sciences, Geology*, vol. 53, No. 3, p. 149-164.

Luusika gravitatsiooni- ja magnetväljaanomaalia uuringud

Kokkuvõtte

Eesti Maaameti poolt 2011. aastal avastatud gravitatsioonivälja kerge Luusika piirkonnas (Idavirumaa) on maksimaalse amplituudiga 6,26 mGal. Aastal 2014 Luusika piirkonnas tehti maapelased Maa magnetväja mõõtmised, mis kinnitasid magnetvälja anomalia olemust ning andsid uusi teadmisi maapões asuva geoloogilise keha magnetilistest omadustest. Antud piirkonda iseloomustas positiivne gravitatsiooni ja magnetvälja anomalia.

Anomaalia allika sügavuse hinnang teostati Bouguer anomalia profiilides kasutades gradientamplituudi ja poollaiuse meetodeid. Anomaalia allika keskpunkti (z) sügavuseks määrati 2500 m ning keha ülemise pinna (z_T) maksimaalsesks sügavuseks 3000 m.

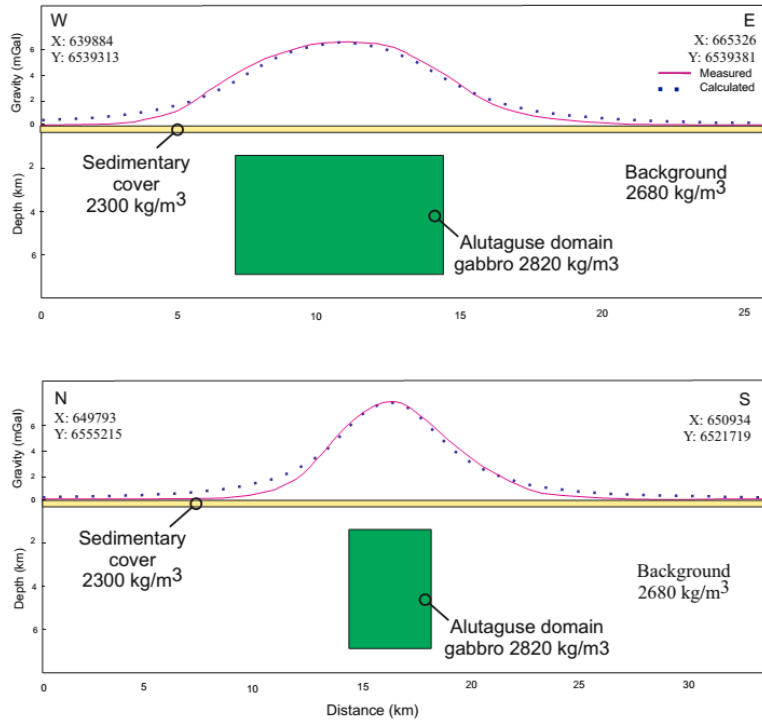
Gravitatsiooni ja magnetvälja profiilidele loodi geoloogilised mudelid. Mudeli eesmärk oli kontrollida Alutaguse domeeni ja postorogeenstete ning anarogeensete kimitite sobivuse anomalia allikaks. Magnetvälja mudeldamisel kasutati vastavat magnetiseerituse suunda. Modelleerimise tulemused on järgmised:

1. Anomaalia allika ülemise pinna sügavus (z_T) varieerub vahemikus 600 ja 1800 m maapinnast.
2. Anomaaliat põhjustava keha tihedus jäääb vahemikku 2760 ... 2920 kg/m³.
3. Luusika keha magnetilise vastuvõtluskuse väärthus on taustkivimiga võrreldes väga kõrge ja jäääb vahemikku $\chi = 20000 \dots 56000 \times 10^{-6}$ SI.

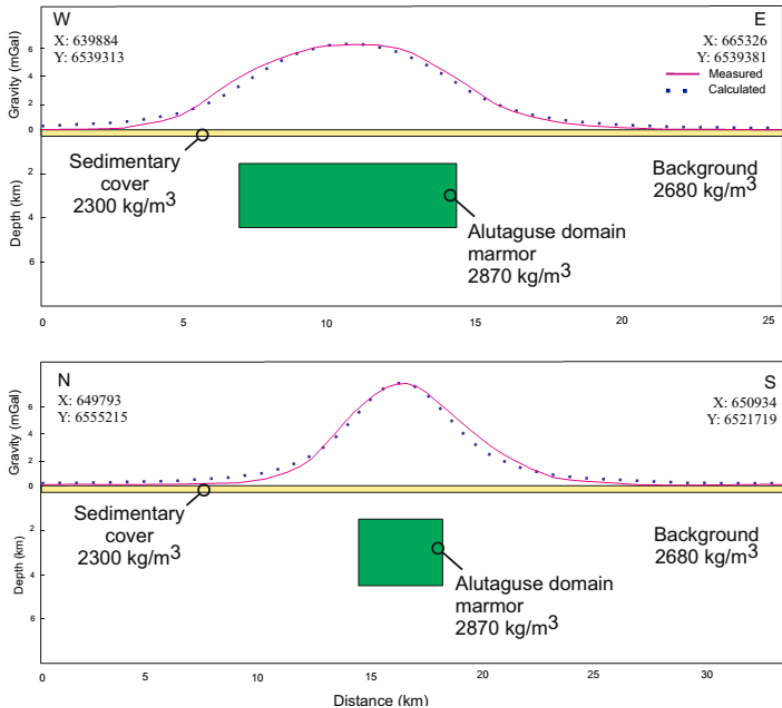
Eesti kristalses aluskorras on sarnaste petrofüüsikaliste omadustega aluselised/keskmised postorogeensed ja anarogeensed massiivid. Teadaolevalt, Luusika anomalia allikas paikneb Kesk-Eesti rikkevööndis, mille läheduses asuvad mõned postorogeensed kvartsmontsoniitsed plutoonid. Seetõttu, Luusika keha võib pidada Taadikverega sarnaseks massiiviks. Samuti on Eesti kristalses aluskorras rapakivigraniitide kompleksi kuuluvad intrusioonid, millega samuti kaasnevad gravitatsiooni- ja magnetvälja anomaliad.

Anomaalia allika modeleerides ja petrofüüsikalisi omadusi võrreldes teostati, et Luusika keha on koostiselt keskmise kuni aluseline kivim, mis sarnaneb Abja, Sigula või Taadikvere massiividega. Lisaks esinemine on tõenäoliselt seotud Kesk-Eesti rikkevööndiga.

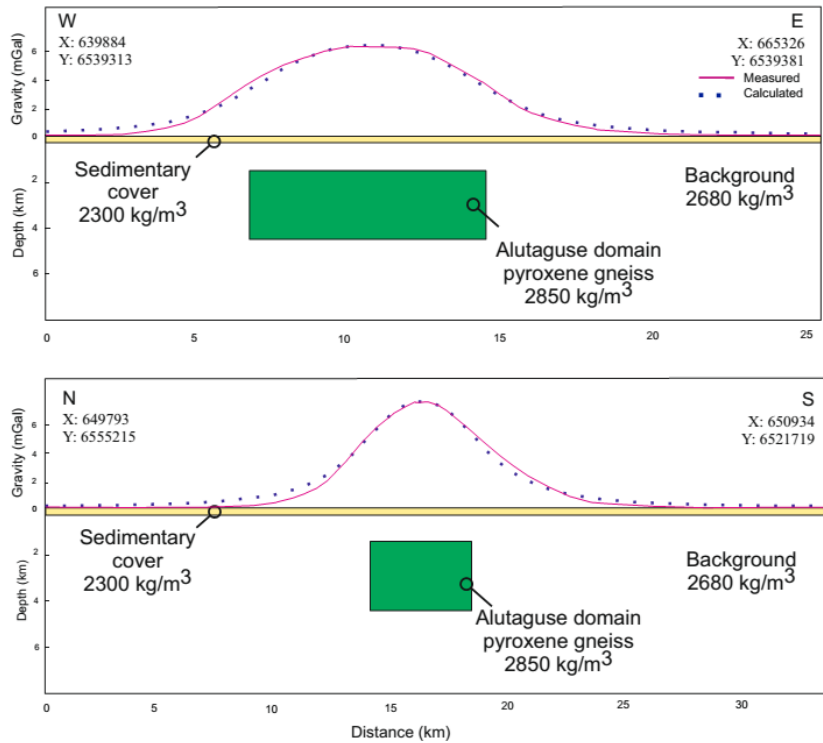
Appendices



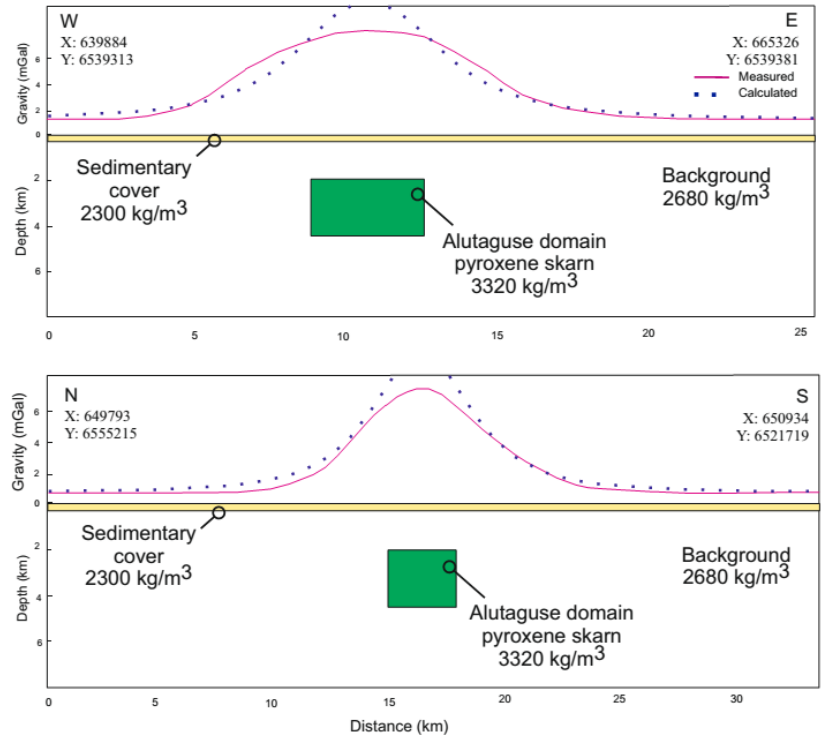
Appendix 1. Gravity profiles (measured and calculated) and cross-sections of Alutaguse domain gabbro-like (green rectangle) model along W-E (upper) and N-S (lower) profiles. The model was accepted and rock type was tested by magnetic modeling.



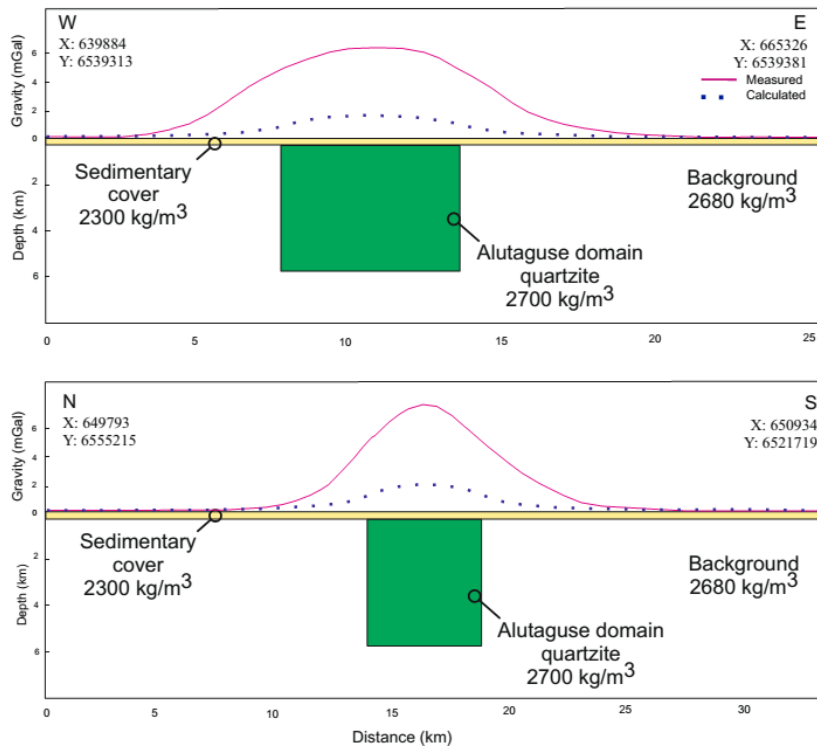
Appendix 2. Gravity profiles (measured and calculated) and cross-sections of Alutaguse domain marmor-like (green rectangle) model along W-E (upper) and N-S (lower) profiles. The model was accepted and rock type was employed during further magnetic modeling.



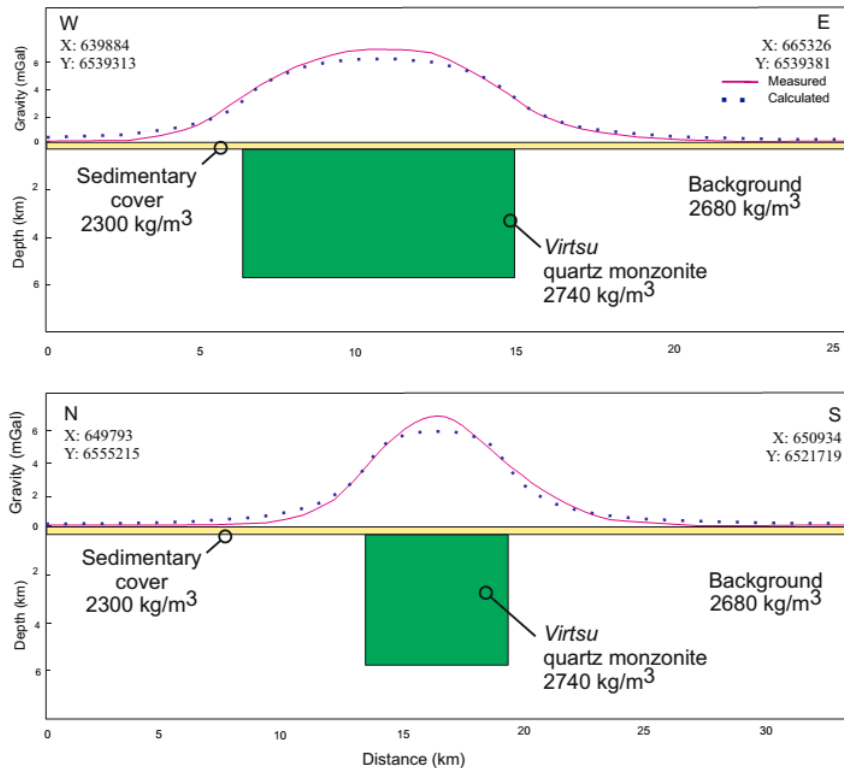
Appendix 3. Gravity profiles (measured and calculated) and cross-sections of Alutaguse domain pyroxene gneiss-like (green rectangle) model along W-E (upper) and N-S (lower) profiles. The model was accepted and rock type was tested by magnetic modeling.



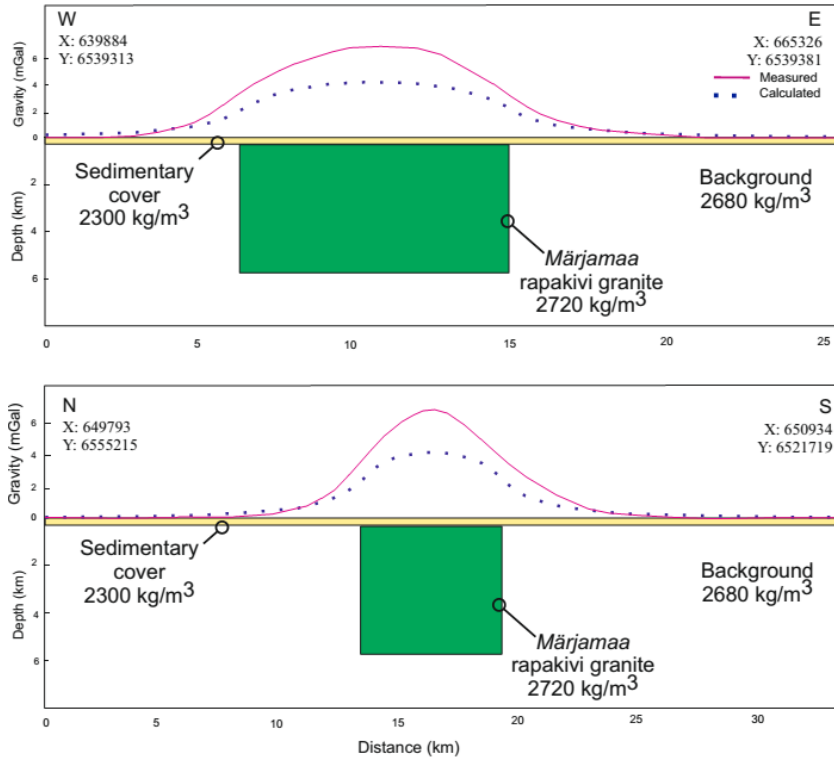
Appendix 4. Gravity profiles (measured and calculated) and cross-sections of Alutaguse domain pyroxene skarn-like (green rectangle) model along W-E (upper) and N-S (lower) profiles. Calculated anomaly exceeded the observed data, and, as a result, model was rejected.



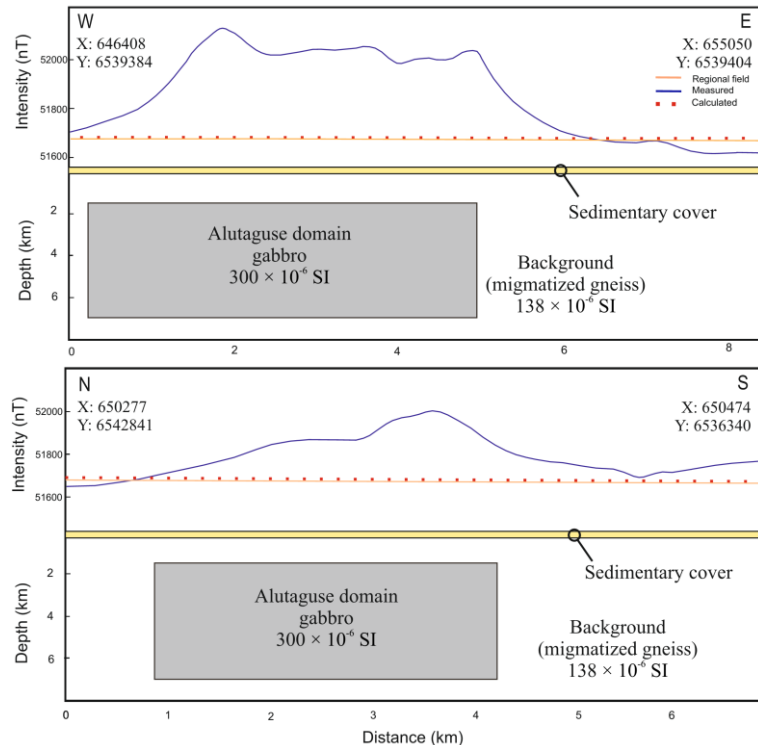
Appendix 5. Gravity profiles (measured and calculated) and cross-sections of Alutaguse domain quartzite-like (green rectangle) model along W-E (upper) and N-S (lower) profiles. The calculated anomaly amplitude is noticeably lower than observed data and the model was rejected.



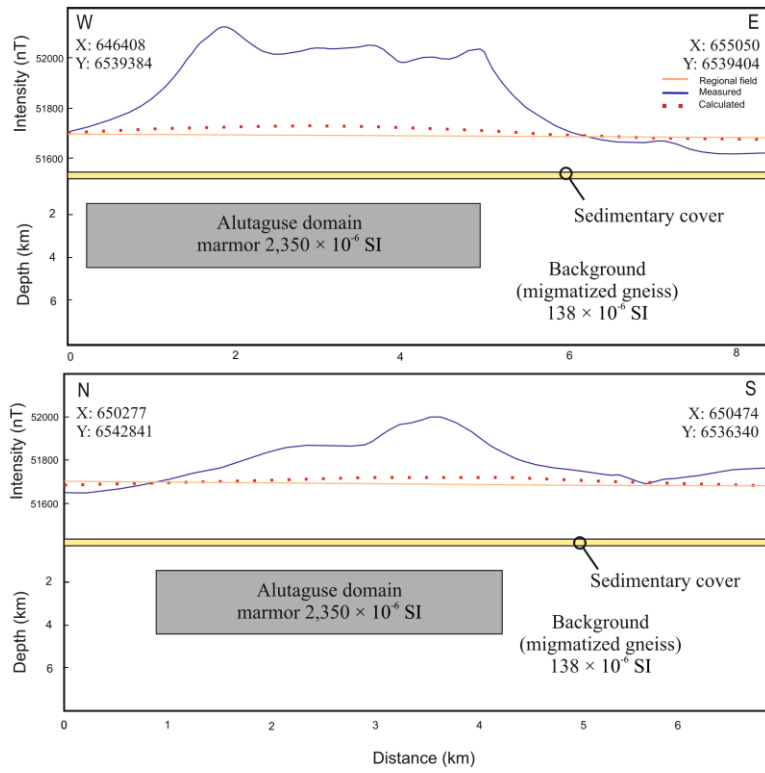
Appendix 6. Gravity profiles (measured and calculated) and cross-sections of Virtsu quartz monzonite-like (green rectangle) model along W-E (upper) and N-S (lower) profiles. The calculated anomaly amplitude is slightly lower than measured data and the model was rejected.



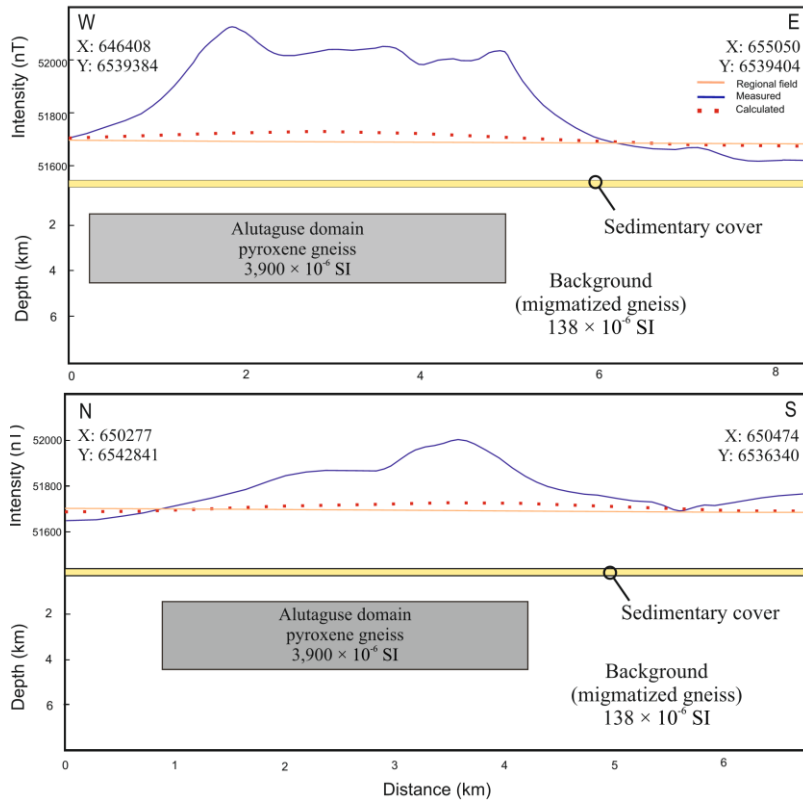
Appendix 7. Gravity profiles (measured and calculated) and cross-sections of Märjamaa (I phase) rapakivi granite-like (green rectangle) model along W-E (upper) and N-S (lower) profiles. The calculated anomaly amplitude is much lower than observed data and the model was rejected.



Appendix 8. Magnetic profiles (measured and calculated) and cross-sections of magnetic Alutaguse domain gabbro-like (grey rectangle) model along W-E (upper) and N-S (lower) profiles. Due to the calculated low magnetic response the model was rejected.



Appendix 9. Magnetic profiles (measured and calculated) and cross-sections of magnetic Alutaguse domain gabbro-like (grey rectangle) model along W-E (upper) and N-S (lower) profiles. Due to the calculated low magnetic response the model was rejected.



Appendix 10. Magnetic profiles (measured and calculated) and cross-sections of magnetic Alutaguse domain pyroxene gneiss-like (grey rectangle) model along W-E (upper) and N-S (lower) profiles. Due to the calculated low magnetic response the model was rejected.

Non-exclusive licence to reproduce thesis and make thesis public

I, Marija Dmitrijeva,

(author's name)

herewith grant the University of Tartu a free permit (non-exclusive licence) to:

1.1. reproduce, for the purpose of preservation and making available to the public, including for addition to the DSpace digital archives until expiry of the term of validity of the copyright, and

1.2. make available to the public via the web environment of the University of Tartu, including via the DSpace digital archives until expiry of the term of validity of the copyright,

“Gravity and magnetic studies of the Luusika potential field anomaly”

(title of thesis)

supervised by Jüri Plado and Tõnis Oja

(supervisor's name)

2. I am aware of the fact that the author retains these rights.

3. I certify that granting the non-exclusive licence does not infringe the intellectual property rights or rights arising from the Personal Data Protection Act.

Tartu 21.05.2015